TITLE OF THE EDITED BOOK: THE WATER-FOOD-ENERGY NEXUS: PROCESSES, TECHNOLOGIES AND CHALLENGES

PUBLISHER: TAYLOR AND FRANCIS

CHAPTER 28

ENVIRONMENTALLY BENIGN BIODIESEL PRODUCTION FROM RENEWABLE SOURCES

SUMAIYA ZAINAL ABIDIN [1,2], BASUDEB SAHA [3,*]

[1]*Faculty of Chemical and Natural Resources Engineering, Universiti Malaysia Pahang, Lebuhraya Tun Razak, 26300 Gambang, Kuantan, Pahang Darul Makmur, Malaysia*

[2]*Center of Excellence for Advanced Research in Fluid Flow, Universiti Malaysia Pahang, Lebuhraya Tun Razak, 26300 Gambang, Kuantan, Pahang Darul Makmur, Malaysia*

[3]*School of Engineering, London South Bank University, London, SE1 0AA, United Kingdom*

**Corresponding author - Tel: +44 (0) 20 7815 7190; Fax: +44 (0) 20 7815 7699; E-Mail: b.saha@lsbu.ac.uk*

TABLE OF CONTENTS

LIST OF FIGURES

LIST OF TABLES

LIST OF ABBREVIATIONS

BET	Brunauer-Emmett-Teller
BSI	British Standard Institution
DVB	Divinylbenzene
FAME	Fatty Acid Methyl Ester
FEG-SEM	Field Emission Gun-Scanning Electron Microscopy
FFA	Free Fatty Acids
FT-IR	Fourier Transform-Infra Red
GC-MS	Gas Chromatography-Mass Spectrometry
PSD	Particle Size Distribution
P-UCO	Pre-treated Used Cooking Oil
RO	Reverse Osmosis
SEM	Scanning Electron Microscopy
SEM-EDX	Scanning Electron Microscopy – Energy Dispersive X-ray
UCO	Used Cooking Oil

28.1 Introduction

Renewable energy has become an important alternative resource in many countries and considered to be potential substitutes to the conventional fossil fuel. In particular, renewable energy in the form of biodiesel is considered to be one of the best available energy resources (Atabani *et al.*, 2012; Liu *et al.*, 2012). As the fuel's feedstock is originated from renewable sources, this type of fuel is well known to be biodegradable and environmental friendly (Kaercher *et al*., 2013). Apart from that, it also owns a good combustion profile, produces less particulates i.e. unburned hydrocarbon and hazardous gases (i.e. carbon monoxide, sulphur dioxide), have a higher cetane number, higher flash point and a higher lubricity (Lin *et al.*, 2011) as compared to conventional diesel. Biodiesel, comprises of monoalkyl esters of fatty acids, is derived from a renewable lipid feedstocks, such as edible oil (i.e. palm, sunflower, soybean) non-edible oils (i.e. jatropha, mahua), animal fats (chicken, lard) and algae. The cost of feedstock alone comprises 75-85% of the overall cost of biodiesel production (Atabani *et al.*, 2012; Abbaszaadeh *et al*., 2012). Currently, the popular feedstocks for biodiesel production is the edible oils however, this was restricted due to the higher price of vegetable oil. The use of vegetable oils in biodiesel production also creates controversial issues on the usage of food elements as the source of fuels.

Cheap, non-edible used cooking oil (UCO) has been found to be an effective feedstock to reduce the cost of biodiesel (Stamenković *et al.*, 2011, Pinzi *et al.*, 2014). According to Balat (2011), UCO is 2.5-3.5 times cheaper than virgin vegetable oils and thus can reduce 60-90% the total production cost of biodiesel (Talebian-Kiakalaieh *et al*., 2013). Yaakob *et al*. (2013) reported that used cooking oil can reduce water pollution and also prevents blockage in water drainage systems. As these feedstocks contain high amount of free fatty acids (FFA) and water, it cannot

be directly used in a base catalysed transesterification reaction. FFA can react with a base catalyst (neutralisation reaction) and accelerates the base catalyst consumption. The high FFA content also causes saponification during the base catalysed transesterification and lowers the yield of biodiesel. Acid catalyst found to have better tolerance to high water and FFA content, whereas the base catalysts, which are very sensitive towards water and FFA are proved to be effective for transesterification of feedstocks with low FFA content. Therefore, high yield could be achieved using a two-step synthesis of biodiesel. A pre-treatment stage (esterification process) is used to reduce the amount of FFA in the feedstock before the reaction proceeds with the base-catalysed transesterification.

The use of heterogeneous catalysts simplifies the production and purification processes because they can be easily separated from the reaction mixture, allowing multiple usage of the catalyst through regeneration process. Among various kinds of acid and base catalysts, ion exchange resins are becoming more popular nowadays because this type of catalyst can catalyse the reactions under mild reaction conditions due to their high concentration of acid/base sites (López *et al.*, 2007). It is an attractive alternative because it is easy to separate and recover from the product mixture. Sulphonated cation exchange resin has been found to be one of the most effective catalysts for esterification of FFA (Tesser *et al.*, 2005; Özbay *et al.*, 2008; Russbueldt and Hoelderich, 2009; Talukder *et al.*, 2009). Few researchers have conducted studies to compare the performance of gelular and macroeticular ion exchange resins. Kouzu *et al.* (2011) conducted a study on the performance of gelular (Amberlyst 31) and macroeticular (Amberlyst 15) matrices for the esterification of soybean oil. It was found that the gelular resin has a higher catalytic activity compared to macroeticular resin as the swelling capacity controls the accessibility of acid sites in the catalyst and it simultaneously affects the overall reactivity. A

contradictory finding was achieved by Feng *et al.* (2010) when they conducted a study on different matrix types of cation exchange resins. Three types of resin were employed in this study, namely the NKC-9 (macroeticular), 001 x 7 (gelular) and D61 (macroeticular). The highest FFA conversion was obtained using NKC-9 and this resin also showed a good conversion in the reusability study. A similar result was reported by Özbay *et al.* (2008) when they investigated the esterification of waste cooking oil using Amberlyst 15, Amberlyst 35, Amberlyst 16 (macroeticular) and Dowex HCR-W2 (gelular) as catalysts; Amberlyst 15 was found to give the highest FFA conversion.

There were also a few studies of the esterification process that focused on the macroeticular cation exchange resins as catalysts. Bianchi *et al.* (2009) studied the de-acidification of animal fats using several types of macroeticular cation exchange resins as catalysts i.e. Amberlyst 15Dry, Amberlyst 36Dry, Amberlyst 39Wet, Amberlyst 40Wet, Amberlyst 46Wet and Amberlyst 70Wet. From this study, more than 90% of the FFA conversion was successfully achieved when Amberlyst 70Wet was used as the catalyst. This catalyst also showed a good conversion rate in the reusability study and performed well even in less severe operating condition (303 K with 1.25 wt% catalyst). Park *et al.* (2008) studied the performance of two different macroeticular cation exchange resin catalysts, Amberlyst-15 and Amberlyst BD20. They found that the amount of pores of the catalyst played an important role, not only in increasing the catalytic activity, but also in reducing the inhibition by water in the esterification process. Study on the comparison between strongly acidic macroporous cation exchange resin (Amberlyst 36) and strongly acidic hypercrosslinked resin (Purolite D5081) has been conducted by Abidin *et al.* (2012). They found that the catalytic performance of the hypercrosslinked sulphonic acid resin was superior to the macroporous catalyst due to the presence of high

specific surface area. Comparison between Purolite D5081 and Novozyme 435 was also studied by Haigh and co-workers (2012, 2013). It was found that Purolite D5081 resin gives higher conversion and negligible side reactions as compared to Novozyme 435. Ilgen (2014) studied on the kinetics and mechanism of oleic acid esterification using Amberlyst 46 as a catalyst. The highest conversion was obtained when the reaction was performed at 3:1 molar ratio of methanol to oleic acid, 100 ºC reaction temperature, 15% catalyst loading in 2 h reaction time. From the kinetic study, Eley Rideal mechanism was found to give the best match to the experimental data and thus, surface reaction was found to be the rate limiting step. Shibasaki-Kitakawa *et al.* (2015) studied continuous production of biodiesel from water rice bran acid oil with 95% of FFA content. The experiment was conducted in a packed column using and PK208LH ion exchange resin as a catalyst. It was found that the concentration of FFA was close to zero after 90 h of reaction. However, a decrease in fatty acid methyl ester (FAME) concentration was detected after 90 h of reaction due to the accumulation of water formed by esterification within the resin. Transesterification of biodiesel is normally conducted using anion exchange resins due to the high time consumption and molar ratio requirement when cation exchange resin is used as catalyst (dos Reis *et al.*, 2005). A comparison study between anion and cation exchange resin has been carried out by Li *et al.* (2012). Four types of ion exchange resins, namely Amberlyst 15 (cation), Amberlite IRC-72 (cation), Amberlite IRA-900 (anion) and Amberlite IRC-93 (anion) have been assessed in the transesterification of yellow horn (Xanthoceras sorbifolia Bunge.) seed oil. Amberlite IRA-900 was reported to have the highest conversion of 96.3%. Amberlyst 15 was also found to give good conversion (83.5%), however, it is still considered a weak catalyst compared to Amberlite IRA-900. Falco *et al.* (2010) also conducted a study on the transesterification of soybean oil using basic and acidic ion exchange resins as catalysts. In this

study, a strongly basic anion exchange resin, BR 1 was reported to give the highest conversion and the selectivity of FAME could potentially reach 100%. Shibasaki-Kitakawa *et al.* (2007) investigated the potential of anion exchange resin as the heterogeneous catalyst. Several types of anion exchange catalysts have been tested for the transesterification of triolein, namely the Diaion PA308, Diaion PA306, Diaion PA306s and HPA 25. Anion exchange resin with a lower cross-linking density and a smaller particle size, Diaion PA306s, was proved to give the highest catalytic activity and resulted in approximately 98.8% purity of biodiesel fuel. In their latest research, Shibasaki-Kitakawa *et al.* (2011) also reported that Diaion PA306s catalyst could act as both catalyst and adsorbent in the transesterification reaction of waste cooking oil with 1% FFA content. He *et al*. (2015) studied the continuous two-stage esterification-transesterification reaction in acidic oil using a combination of cation (NKC-9) and anion (D261) exchange resins as catalysts. The reaction was found to convert 95.1% of the acidic oil (combination of oleic acid and soybean oil) to biodiesel. Furthermore, the biodiesel product was also found to meet the biodiesel standard requirement of Chinese Standard.

This chapter concentrates on the production of biodiesel from UCO using two-stage esterification-transesterification catalytic reactions with ion exchange resins as catalysts. This work was conducted in collaboration with Purolite International Limited for possible commercialisation of novel Purolite ion exchange resins as potential biodiesel production catalysts. The influence of the following reaction parameters i.e. mass transfer resistance, catalyst loading, reaction temperature, methanol to oil feed mole ratio and reusability of catalyst were investigated.

28.2 Materials and Method

28.2.1 Materials

The UCO was supplied by Greenfuel Oil Company Limited, UK with the acid value of 12 mg KOH/g oil. Ion exchange resin catalysts (Purolite CT-122, Purolite CT-169, Purolite CT-175, Purolite CT-275 and Purolite D5081, Purolite D5082) were supplied by Purolite International Limited (UK), Diaion PA306s was supplied by Mitsubishi Chemicals (Japan) and Amberlyst 36 was purchased from Sigma Aldrich, UK. All resins were supplied in wet form. Methanol (>99.5% purity), sodium hydroxide (98+%) pellets, 0.1 M standardised solution acid hydrochloric, 0.1 M standardised solution sodium hydroxide, 0.1 M standardised solution sodium hydroxide in 2-propanol, toulene (99.5%), 2-propanol (99+%), glacial acetic acid (99.85%), chloroform (>99%), sodium chloride, phenolphthalein, iso-octane (>99.5) and acetonitrile (>99.8%) were purchased from Fisher Scientific, UK and *p*-naphtholbenzein, *n*-hexane, methyl heptadecanoate (>99%), methyl linoleate (>99%), methyl linolenate (>99%), methyl oleate (>99%), methyl palmitate (>99%) and methyl stearate (>99%) were purchased from Sigma Aldrich, UK.

28.2.2 Catalyst Preparation

Two types of resins were used in this research work i.e. cation exchange resin and anion exchange resin. All of these resins were supplied in wet form. Purolite CT-122, Purolite CT-169, Purolite CT-175, Purolite CT-275, Amberlyst 36, Purolite D5081 and Purolite D5082 are classified as strongly acidic cation exchange resins, whereas Diaion PA306s is classified as a strongly basic anion exchange resin, supplied in chloride form. These resins were pre-treated before being used as the reaction catalysts. For cation exchange resin, all resins were immersed

in methanol overnight and pre-treated with methanol in an ultrasonic bath. The process takes few cycles of rinsing to ensure that all contaminants were removed. The conductivity of the residual solution was recorded and the process continued until the conductivity of the residual solution was approximately the same with the solvent. Finally, the resins were dried in a vacuum oven at 373 K for 6 h to remove any water and methanol. The dried catalyst was kept in a sealed bottle prior to use. The anion exchange resin, Diaion PA306s was prepared prior to use. It was mixed with 1 M of sodium hydroxide (NaOH) to displace the chloride ions to hydroxyl ions. After that, the resin was washed with reverse osmosis (RO) water. During this washing process, the conductivity of the residual solution was recorded and the process continued until the conductivity of the residual solution was approximately the same as the RO water. The catalyst was then rinsed with methanol, filtered and decanted and left overnight in a closed environment.

28.2.3 Catalyst Characterisation

Elemental analysis was performed using a Thermoquest EA1110 Elemental Analyser. The sulphur determination was carried out separately using an oxygen flask combustion analysis, followed by a titration. All the results are reported in weight percentage of carbon, hydrogen, nitrogen and sulphur. Oxygen cannot be measured by elemental analysis and therefore, the percentage of oxygen content was determined by the difference from the total weight percentage of other elements (i.e. carbon, hydrogen, nitrogen and sulphur). The true density (ρ_t) was measured using a Micromeritics Helium Pycnometer 1305. The true density of particles was determined using the standard density formula. A Carl Zeiss (Leo) 1530 VP) field emission gun-scanning electron microscope (FEG-SEM), Scanning Electron Microscopy (SEM) and Scanning Electron Microscopy – Energy Dispersive X-ray (SEM-EDX) were used to study the

morphology of the catalysts and to determine the elemental composition. Surface area, pore volume and average pore diameter were determined from adsorption isotherms using a Micromeritics ASAP 2020 surface area analyser. The samples were degassed using two-stage temperature ramping under a vacuum of <10 mm Hg, followed by sample analysis at 77 K using nitrogen gas. Table 28.1 shows the elemental analysis results for ion exchange resin catalysts. There was unexpected presence of nitrogen in some of the cation exchange resins, and the value was less than 1%. In this case, nitrogen was assumed to be a contaminant in the sample. Table 28.2 shows the summarized chemical and physical properties of catalysts used in transesterification process.

Table 28.1 The elemental analysis results for ion exchange resin catalysts**

Catalyst	% C	% H	% N	% S	% O*
Amberlyst 36	41.18	4.10	0.10	18.27	35.35
Diaion PA306s	55.59	9.42	4.34	0.00	30.65
Purolite CT-122	51.06	5.68	0.06	15.99	27.22
Purolite CT-169	48.88	5.07	0.06	16.58	29.42
Purolite CT-175	47.35	4.74	0.00	15.75	32.17
Purolite CT-275	44.59	4.61	0.00	16.61	34.20
Purolite D5081	77.04	5.32	0.95	4.09	12.61
Purolite D5082	68.87	4.44	0.13	5.92	20.65

*Oxygen by difference

**Adapted with permission from Abidin et al., 2012, Industrial and Engineering Chemistry Research, 51: 14653–14664, American Chemical Society.

Table 28.2 Physical and chemical properties of catalysts used for esterification and transesterification process**

Catalyst Properties	**Amberlyst 15**	**Diaion PA306s**	**Purolite CT-122**	**Purolite CT-169**	**Purolite CT-175**	**Purolite CT-275**	**Purolite D5081**	**Purolite D5082**
Physical Appearance	Opaque spherical beads	White beads	Golden spherical beads	Opaque spherical beads	Opaque spherical beads	Opaque spherical beads	Opaque spherical beads	Opaque spherical beads
Functional Group	Sulfonic acid	Quaternary ammonium	Sulfonic acid	Sulfonic acid	Sulfonic acid	Sulfonic acid	Sulfonic acid	Sulfonic acid
Moisture Capacity (%H^+)*	52-57	66 - 76	78 - 82	51 - 57	50 - 57	51 - 59	56.9	56.2
Polymer structure	Macroporous Polystyrene cross-linked DVB	Gelular Polystyrene cross-linked DVB	Gelular Polystyrene cross-linked DVB	Macroporous Polystyrene cross-linked DVB	Macroporous Polystyrene cross-linked DVB	Macroporous Polystyrene cross-linked DVB	Macroporous Polystyrene cross-linked DVB	Macroporous Polystyrene cross-linked DVB
Cross-linking level	Medium cross-linked	Low cross-linked	Low cross-linked	Medium cross-linked	Highly cross-linked	Highly cross-linked	Hyper-crosslinked	Hyper-crosslinked
Temperature limit (K)*	393	333	403	393	418	418	393	393
Specific Surface Area (m^2g^1)	53	#	#	37.97	23.77	20.9	514.18	459.62
Total Pore Volume ($cm^3\ g^{-1}$)	0.4	#	#	0.27	0.108	0.108	0.47	0.36
Average pore diameter (nm)	30	#	#	27.42	17.37	19.6	3.69	3.14
True Density ($g\ cm^{-3}$)	1.027	1.297	1.297	1.297	1.296	1.296	1.309	1.373

*Manufacturer data, #Data could not be measured

**Adapted with permission from Abidin et al., 2012, Industrial and Engineering Chemistry Research, 51: 14653–14664, American Chemical Society.

28.2.4 Average Molecular Mass Determination: Analysis of Fatty Acid Composition in the UCO

The fatty acids bonded to the glycerine backbone vary depending on the oil type and as a result an average molecular mass is generally determined based on the fatty acid composition of the oil. Average molecular mass was calculated by multiplying the mass fractions of fatty acids presence in the oil with the individual molecular mass of each fatty acid involved. The determination of fatty acid composition was done by converting the triglycerides to glycerine and FAME through a methylation or hydrolysis process (David *et al*., 2005). Derivatisation through the methylation process has been widely used to characterise lipid fractions in fats and oil (Dowd, 1998; Knothe and Steidley, 2009). It is a well-accepted characterisation method because of the robustness and reproducibility of the chromatographic data. These methods are also cheaper in terms of reagent usage and do not require expensive equipment.

In this study, the sample was prepared using methods in European Union (EU) Regulation (EU Regulation, 1991) and the results were verified using British Standard Institution (BSI) standard method (EN ISO 12966-2, 2011). Derivatisation process begins by weighing 100 mg of UCO in a 20 mL screw-cap test tube or reaction vial. Then, the UCO was dissolved in 10 mL of n-hexane. 100 µL of 2N potassium hydroxide was added to the reaction vial together with 100 mL of methanol. The tube or vial was closed and mixed vigorously for 60 seconds. The sample was then transferred into a conical bottom tube for centrifugation process. This process takes about 10 minutes with 16000 rpm rotational speed. The upper layer, the clear supernatant was analysed by gas chromatography – mass spectrometry (GC-MS).

28.2.5 Esterification-Transesterification Reaction

The esterification process was carried out in a four-neck 1000 mL cylindrical jacketed-glass reactor, equipped with a mechanical stirrer, sampling outlet and reflux condenser to prevent the loss of reactant due to vaporisation. Heating was achieved by circulating water from a water bath and through the reactor and a thermocouple was used for temperature monitoring. Figure 28.1 shows the experimental set-up of the reaction process and Figure 28.2 shows the reaction scheme of the esterification process.

A specified amount of UCO and methanol was added to the reactor and the stirring and heating of the reaction mixtures were started. When the reactor reached the required temperature, catalyst was added and this point was taken as the zero time for the reaction. The samples were periodically taken from the reactor for FFA analysis. After 8 h, the reaction mixture was transferred to a separation funnel and allowed to settle overnight to form two layers; the top layer consisted of excess methanol and its impurities whereas the bottom layer was mainly unreacted UCO together with traces of methanol, glycerine, esters and the remaining catalyst. The bottom layer was withdrawn from the separating funnel together with the catalyst and the retained catalyst was washed, dried and stored for further experimental work. Studies on the mass transfer resistance as well as the effect of methanol to UCO molar ratio, catalyst loading and reaction temperature has been conducted. In addition, a blank run without catalyst has been performed and there was no conversion of FFA after 8 h of reaction time. Therefore, it was concluded that the esterification of FFA occurs only due to the presence of the catalyst. The product from the esterification process is called as pre-treated used cooking oil (P-UCO). The P-UCO was used as the raw material for transesterification process. Figure 28.3 shows the reaction scheme of the transesterification process. The experimental set-up and procedure for

transesterification was similar to the esterification, except that the size for transesterification reactor was smaller i.e. 250 mL. Studies on the mass transfer resistance as well as the effect of methanol to UCO molar ratio, catalyst loading and reaction temperature have been conducted. Samples were taken periodically from the reactor for FAME analysis using GC-MS. The results were used to determine triglycerides conversion. Once the experiment was completed, the reaction mixture was separated from the spent catalyst, transferred to a separating funnel and allowed to settle overnight. The FAME-rich phase (unpurified biodiesel) was withdrawn from the separating funnel and introduced to a rotary evaporator to remove traces of methanol, followed by washing process. Finally, the purified biodiesel was separated from the washing agent and stored for further analysis. In terms of the reproducibility of the experimental data, selected experiments were repeated 3 times and it was found that there was ±2% difference in the results. Therefore, it was assumed that a similar error applies to all results.

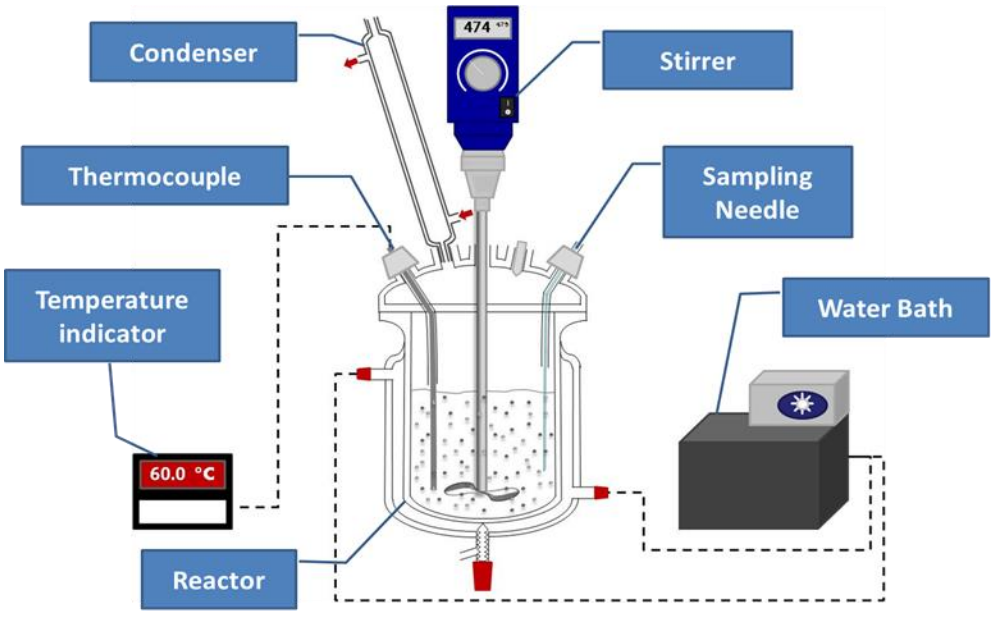

Figure 28.1 Experimental set-up for the reaction process**.

**Adapted with permission from Abidin et al., 2012, Industrial and Engineering Chemistry Research, 51: 14653–14664, American Chemical Society.

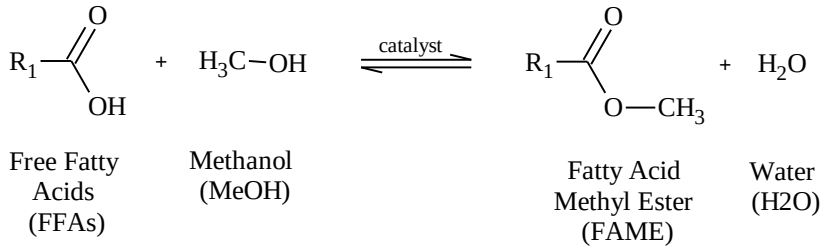

Figure 28.2 Reaction scheme for the esterification process: Conversion of FFAs to FAME. R_1 represents the fatty acid group**.

**Adapted with permission from Abidin et al., 2012, Industrial and Engineering Chemistry Research, 51: 14653–14664, American Chemical Society.

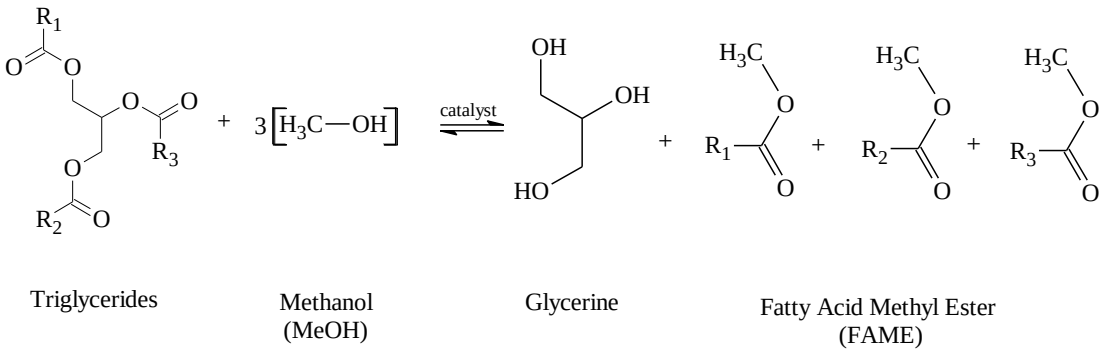

Figure 28.3 Reaction scheme for the transesterification process. R_1, R_2 and R_3 represent the fatty acids group attached to the backbone of triglycerides**.

**Adapted with permission from Abidin et al., 2012, Industrial and Engineering Chemistry Research, 51: 14653–14664, American Chemical Society.

28.2.6 Catalyst Reusability Study

A reusability study of was conducted to determine the catalyst life span. For esterification process, used catalyst was washed with methanol with the aid of an ultrasonic bath until there were no traces of oil and colorless solution were obtained. During this washing process, the conductivity of the residual solution was recorded and the process continues until the conductivity of the residual solution is approximately the same with the solvent (methanol). The

washed catalyst was filtered and dried in a vacuum oven at 100 ˚C for 6 h. The reusability study was carried out under the optimum process conditions. The fresh and used catalysts were tested for SEM, SEM-EDX, acid capacity and elemental analyses. An investigation into the homogeneous contribution was carried out to establish if sulphonic acid groups were leached during the reaction process. The process flow diagram for the reusability study is summarized in Figure 28.4. It was done by reacting fresh methanol with unused pre-treated catalyst for 8 h at 60ºC and 475 rpm stirring speed. After that, the catalyst was filtered and the solution was used in the subsequent reaction with fresh UCO (6:1 (methanol:UCO) molar ratio), in the absence of any catalyst. This is referred to as the first cycle of homogeneous contribution study. The filtered catalyst was dried in the vacuum oven for 6 h (100°C) and this catalyst was then used for an experiment with fresh methanol and fresh UCO at optimum condition to monitor the conversion trend as a result of the catalyst being treated with methanol. This result was plotted as the first cycle of methanol treated catalyst study.

The spent catalyst from the previous methanol treated catalyst experiment was washed thoroughly with methanol using ultrasonic bath until there were no evidence of UCO contamination. The catalyst was filtered and dried in a vacuum oven at 100ºC for 6 h. The experimental work proceeded to the second homogeneous cycle, where the reaction took place between the fresh methanol and used catalyst. The used catalyst was the same catalyst used in the first cycle of homogeneous contribution study and the first cycle of methanol treated catalyst study. The filtered solution from the methanol-catalyst reaction was added to fresh UCO (6:1 (methanol:UCO) molar ratio) without the presence of catalyst and the FFA conversion was monitored. The result was plotted as the second cycle of homogeneous contribution study. The used catalyst obtained from the methanol-catalyst reaction was dried (100ºC, 6 h) and introduced

to fresh UCO and fresh methanol. By using the optimum reaction parameters, the esterification was conducted and the second cycle of methanol treated catalyst data was plotted.

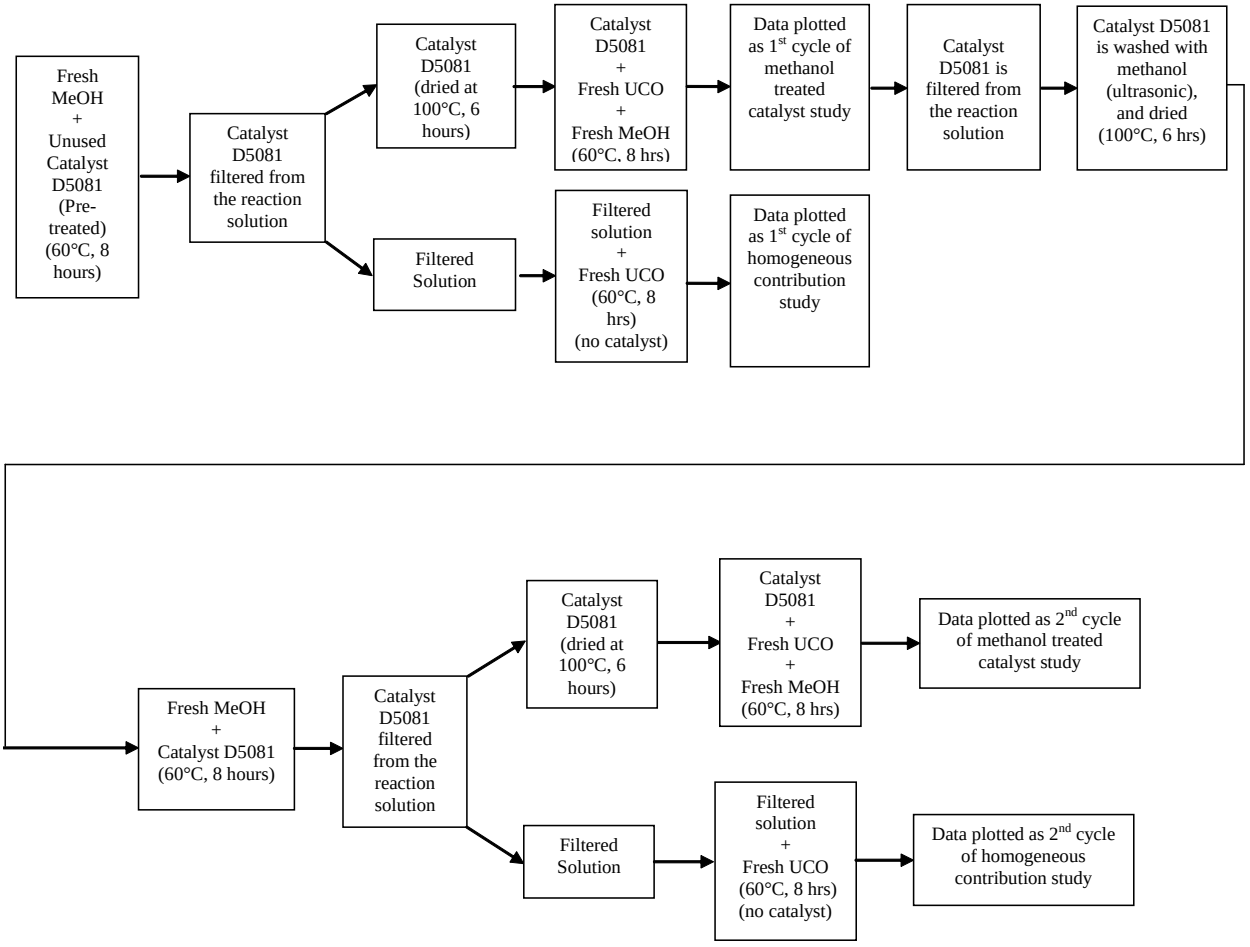

Figure 28.4 Process flow diagram for catalyst reusability study**.

**Adapted with permission from Abidin et al., 2012, Industrial and Engineering Chemistry Research, 51: 14653–14664, American Chemical Society.

A slightly different approach was carried out for anion exchange resin used in transesterification reaction. The used catalyst was washed with glacial acetic acid in methanol to displace the fatty acid ions. This displacement step was conducted with the aid of an ultrasonic bath until there were no traces of P-UCO and a colourless solution was obtained. The catalyst was then washed using RO water to remove excess of acetic acid solution. The catalyst was mixed with 1 M

NaOH to displace the acetate ions with hydroxyl ions, followed by washing with RO water to remove excess NaOH solution. During this washing process, the conductivity of the residual solution was recorded and the process continued until the conductivity of the residual solution was approximately the same as the RO water. The catalyst was rinsed with methanol, filtered and decanted overnight in a closed environment.

28.2.7 GC-MS analysis

The FAME content was assayed using a Hewlett Packard GC-MS model HP-6890 and HP5973 (mass selective detector). A DB-WAX (J & W Scientific) capillary column of length 30 m and internal diameter of 0.25 x 10^{-3} m packed with polyethylene glycol (0.25 μm film thickness) was used. Helium was used as a carrier gas at a constant flow rate of 1.1 mL min^{-1}. The temperature of both the injector and the detector was set at 523 K. The injection volume of 1 μL and a split ratio of 10:1 were used as part of the GC-MS analysis method. The initial oven temperature was held at 343 K for 2 min after the sample injection. The oven temperature was then ramped from 343 – 483 K at a rate of 40 K min^{-1} and from 483 – 503 K at a rate of 7 K min^{-1}. The oven temperature was held at 503 K for 11 min to remove any remaining traces of the sample. The total run time for each sample was approximately 19.5 min. The detailed analysis experimental procedure has been published by Abidin *et al.* (2013). The determination of monoglycerides, diglycerides and triglycerides in the UCO were carried out using the method established by Haigh *et al.* (2014).

28.3 Results and Discussions

28.3.1 GC-MS Analysis of Derivatised UCO

Figure 28.5 shows a typical chromatogram of the derivatised UCO. From the chromatogram, six different components (including the reference standard) were identified. The retention time for each individual component are as follows; methyl palmitate (C16:0) appeared at 8.324 min retention time, methyl heptadecanoate (C17:0 - reference standard) at 8.950 min, methyl stearate (C18:0) at 9.712 min, methyl oleate (C18:1) at 9.914 min, methyl linoleate (C18:2) at 10.349 min and finally methyl linolenate (C18:3) at 11.005 min. As methylation process converts fatty acids to methyl esters through derivatisation method, it could be concluded that there was 5 main components presence in UCO, namely the palmitic acid, stearic acid, oleic acid, linoleic acid and linolenic acid.

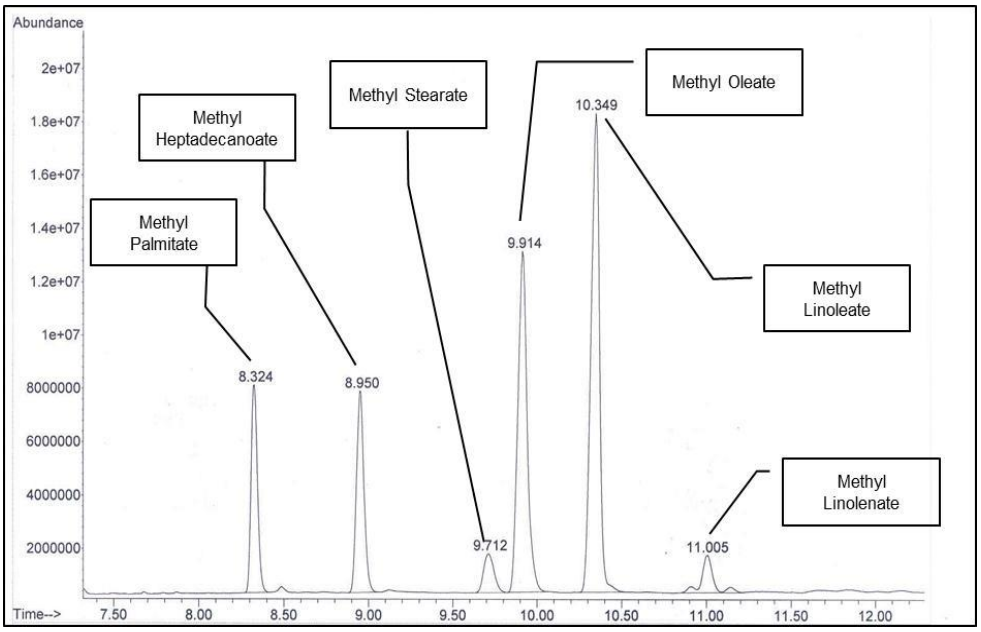

Figure 28.5 Chromatogram of the derivatised UCO**.

**Adapted with permission from Abidin et al., 2012, Industrial and Engineering Chemistry Research, 51: 14653–14664, American Chemical Society.

The response factor for each component was determined using the calibration of individual standards. The pre-determined response factor was then used to determine the fatty acid composition of the sample. By calculating the mass fractions of each fatty acid, the average molecular mass of the fatty acids could be easily calculated and will be further used to determine the methanol to UCO molar ratio (Zhang and Jiang, 2008). The fatty acids composition is summarized in Table 28.3. This data clearly shows that oleic and linoleic acids comprise more than 80% of the total fatty acids in the sample. Using the European Union (EU) Regulation method, the average molecular mass of fatty acids is 278.11 g/mol. The reliability of the previous standard method was verified by analyzing the sample according to the BSI method, EN ISO 12966-2 (2011). It was found that the results were very similar and the average molecular mass of fatty acids obtained using the second method was 277.93 g/mol. Therefore, it can be concluded that both methods are comparable.

Table 28.3 Percentage composition of fatty acid in the UCO**

Component	% Composition (w/w)
Palmitic acid (C16:0)	11.34
Stearic acid (C18:0)	3.18
Oleic acid (C18:1)	43.95
Linoleic acid (C18:2)	36.44
Linolenic acid (C18:3)	5.09

**Adapted with permission from Abidin et al., 2012, Industrial and Engineering Chemistry Research, 51: 14653–14664, American Chemical Society.

28.3.2 Esterification Reaction

28.3.2.1 *Catalysts Screening Study*

In order to identify the best of the three ion exchange resins for further experimental work, all three resins, namely Purolite D5081, Purolite D5082 and Amberlyst 36 were evaluated under the same reaction conditions, i.e. at 1% (w/w) of catalyst loading, 6:1 methanol to UCO molar ratio,

60°C reaction temperature and 350 rpm impeller stirring speed. From Figure 28.6, it can be seen that, after 8 h, Purolite D5081 resin achieved the highest FFA conversion of ~88%, while Purolite D5082 and Amberlyst 36 achieved FFA conversion of ~78% and ~44%, respectively. The differences in the properties of various resins i.e. surface area measurement, elemental analysis and acid capacity analysis can be used to explain the differences in catalytic activity (Table 28.4 and Table 28.5). These analyses show that even though Purolite D5081 has the lowest sulphur content (Table 28.4), it exhibits the highest specific surface area and total pore volume, which means that there are more accessible active sites for the reaction to occur and hence reaches equilibrium at a faster. In addition, the particle size distribution results (Figure 28.7) show that Purolite D5081 has the smallest average particle size, which leads to a larger external surface area compared to the other resins. A larger surface area may contribute to a faster rate of reaction and shorten the time to reach equilibrium however these catalysts are highly porous. As a result this is effect very small when compared to the effect of the pore volume.

Although Amberlyst 36 has the highest sulphur content and the largest average pore diameter, the result from the esterification reaction (Figure 28.6) shows that Amberlyst 36 has the lowest conversion as compared to Purolite D5081 and D5082 resins. This is because Amberlyst 36 has the lowest specific surface area and lowest pore volume compared to the Purolite resins and, therefore, there are less active catalytic sites available for the reaction to occur. The level of divinylbenzene (DVB) cross-linking also contributes significantly to the level of FFA conversion. From Figure 28.6, it could be seen that resins with high DVB cross-linking (Purolite D5081 and D5082) results in higher FFA conversion compared with lower DVB cross-linking resin (Amberlyst 36). The Fourier Transform-Infra Red (FT-IR) analysis has also been carried

out and there was no noticeable change of functional groups for all the resin samples and therefore, these results are not presented in the paper. The FT-IR results also indicate that sulphur was present only in sulphonic acid functional group. Since Purolite D5081 showed the best catalytic performance, it was used for further experimental work.

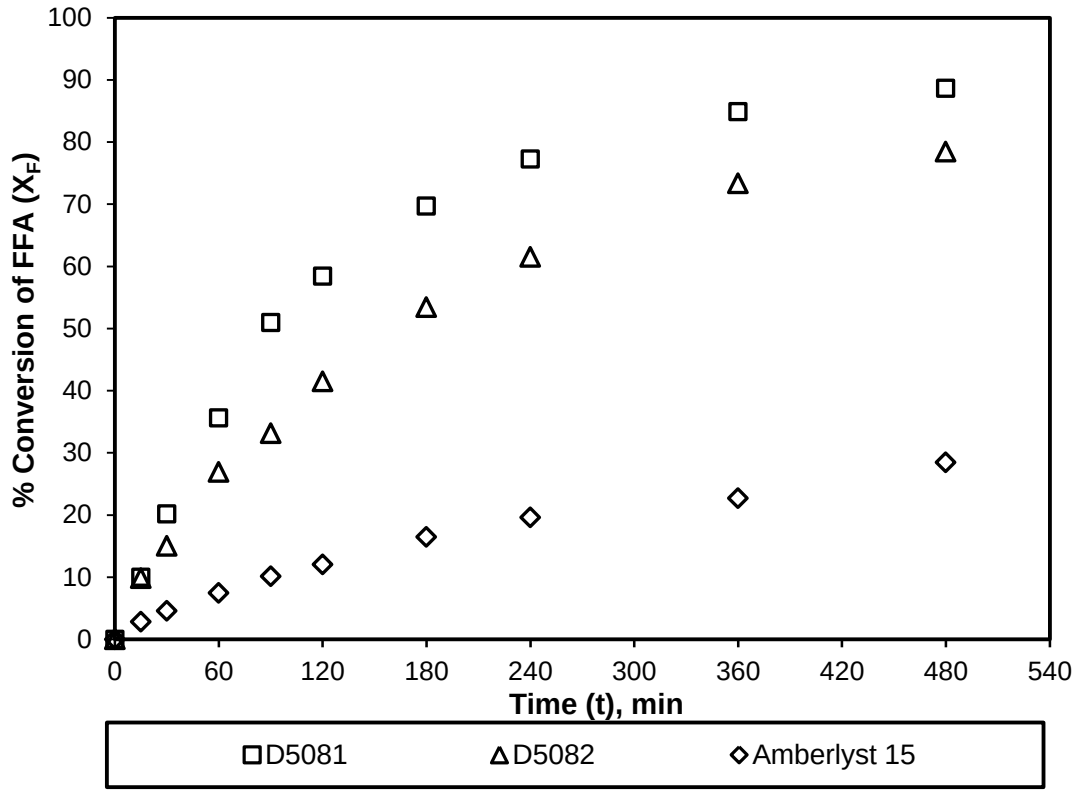

Figure 28.6 Effects of different types of ion exchange resins on FFA conversion. Experimental conditions: molar ratio (methanol:UCO): 6:1; catalyst loading: 1% (w/w); stirring speed: 350rpm; reaction temperature: 60ºC**.

**Adapted with permission from Abidin et al., 2012, Industrial and Engineering Chemistry Research, 51: 14653–14664, American Chemical Society.

Table 28.4 Elemental Analysis for fresh and used ion exchange resins**

Catalyst	% C	% H	% N	% S	% O*
Fresh D5081	77.04	5.32	0.95	4.09	12.61
Used D5081 **	77.41	5.69	0.93	3.32	12.66
Fresh D5082	68.87	4.44	0.13	5.92	20.65
Used D5082**	69.07	4.53	0.03	5.41	20.97
Fresh Amberlyst 36	42.18	4.10	0.10	18.27	35.35
Used Amberlyst 36**	42.18	4.19	0.10	18.17	35.36

All the percentages are in w/w %, *Oxygen by difference, **Washing after 1st cycle reaction

**Adapted with permission from Abidin et al., 2012, Industrial and Engineering Chemistry Research, 51: 14653–14664, American Chemical Society.

Table 28.5 Acid capacity for fresh and used ion exchange resins**

Catalyst	Fresh Resin (mmol/g)	Used Resin (mmol/g)
D5081	1.59	1.39
D5082	1.79	1.59
Amberlyst 36	5.00	4.99

**Adapted with permission from Abidin et al., 2012, Industrial and Engineering Chemistry Research, 51: 14653–14664, American Chemical Society.

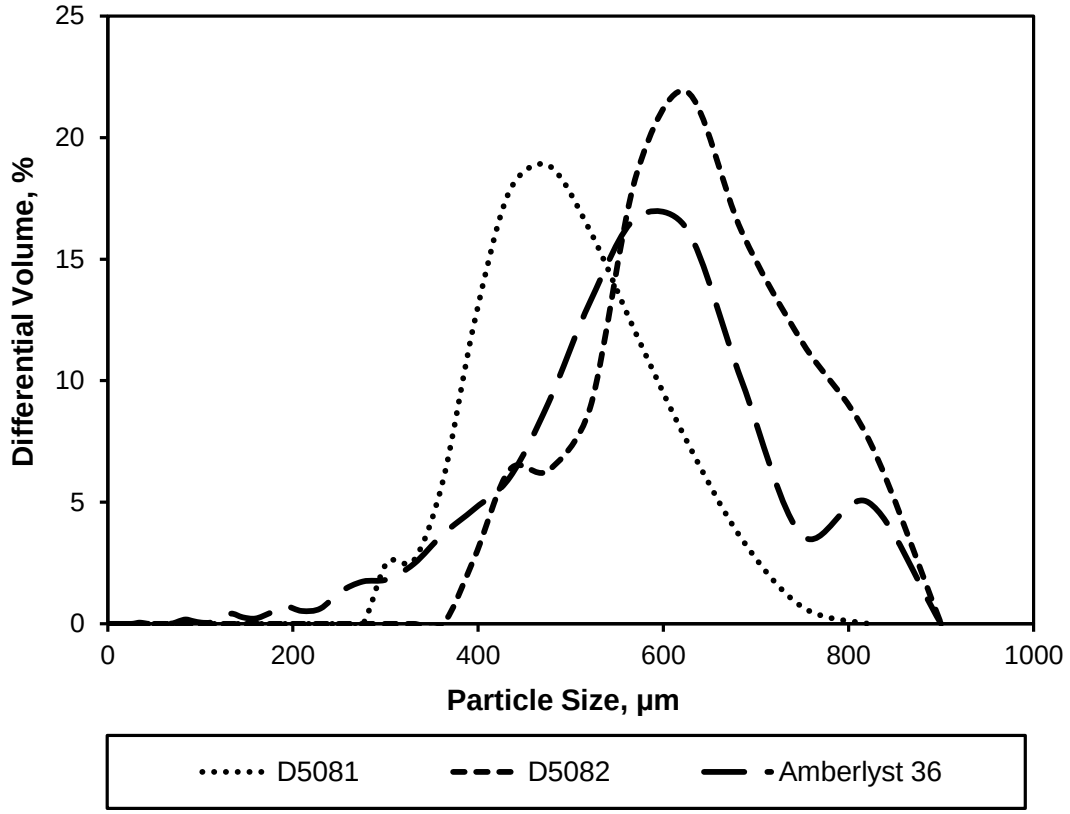

Figure 28.7 Particle size distribution of ion exchange resins catalysts**.

**Adapted with permission from Abidin et al., 2012, Industrial and Engineering Chemistry Research, 51: 14653–14664, American Chemical Society.

28.3.2.2 *Investigation on the Effect of Mass Transfer Resistance in Esterification Reaction*

There are two types of mass transfer resistances involved in ion exchange catalysis. The first is external mass transfer resistance, which takes place across the solid-liquid interface while the second is the internal mass transfer resistance, associated with the differences in particle size distribution of the catalysts. Mixing is one of the key factors to optimise the production of biodiesel as it increases the interaction between the reactants (methanol and UCO) and the catalyst, predominantly at the early stage of the reaction. However, after the reaction mixture reaches the stage where the reactant and the catalyst are well-mixed (e.g. there is sufficient

contact between the catalyst and the reactant), there is no additional benefit from increasing the stirring speed. This phenomenon is due to the external mass transfer resistances.

In order to investigate the influence of external mass transfer resistance, three different stirring rates were investigated for the reaction process and the conversion patterns were observed. Figure 28.8 shows the trend for FFA conversion of Purolite D5081 for three levels of impeller agitation speed, i.e. 350, 475 and 600 rpm. The FFA conversion between the selected stirring rates gave almost an identical trend with less than 2% difference when the agitation speed increased from 350 rpm to 600 rpm. As the stirring speed only has a small impact on the FFA conversion, it was confirmed that there was no evidence of external mass transfer resistance in the esterification reaction.

Internal mass transfer resistance refers to resistance of movement of reactant inside the pores of the catalyst. In order to investigate the occurrence of internal mass transfer resistance, a set of experiments was conducted using various ranges of particle sizes. Figure 28.9 shows the effect of different particle size distribution (PSD) on the FFA conversion. From Figure 28.9, it can be seen that 280-800 μm particle range gives a slightly higher conversion compared to the other two particle ranges. This is because this range i.e. 280-800 μm covers a wide range of particles and therefore the possibility of having smaller particles is higher. This leads to a higher conversion of FFA as smaller particles have shorter pore channels and a larger area of the pores is accessible by the reactant molecules. To support this argument, a comparison was made between 600-710 and 425-500 μm range and it was found that the conversion for 600-710 μm particle size was slightly lower than 425-500 μm particle size in the first 5 h of reaction. Nevertheless, the final conversions of FFA for all three particle ranges were approximately the same at the end of 8 h reaction. This finding proved the previous theory of smaller particles contributing to a larger

accessible surface area and thus increasing the FFA conversion. However, the difference between each range was very small (less than ±2%) and the final conversions were approximately the same. Therefore the effect of internal mass transfer limitation can be eliminated. As a conclusion, stirring speed of 350 rpm and above was selected for subsequent experiments as there was no external mass transfer resistance above this speed limit and the Purolite D5081 resin is used without sieving.

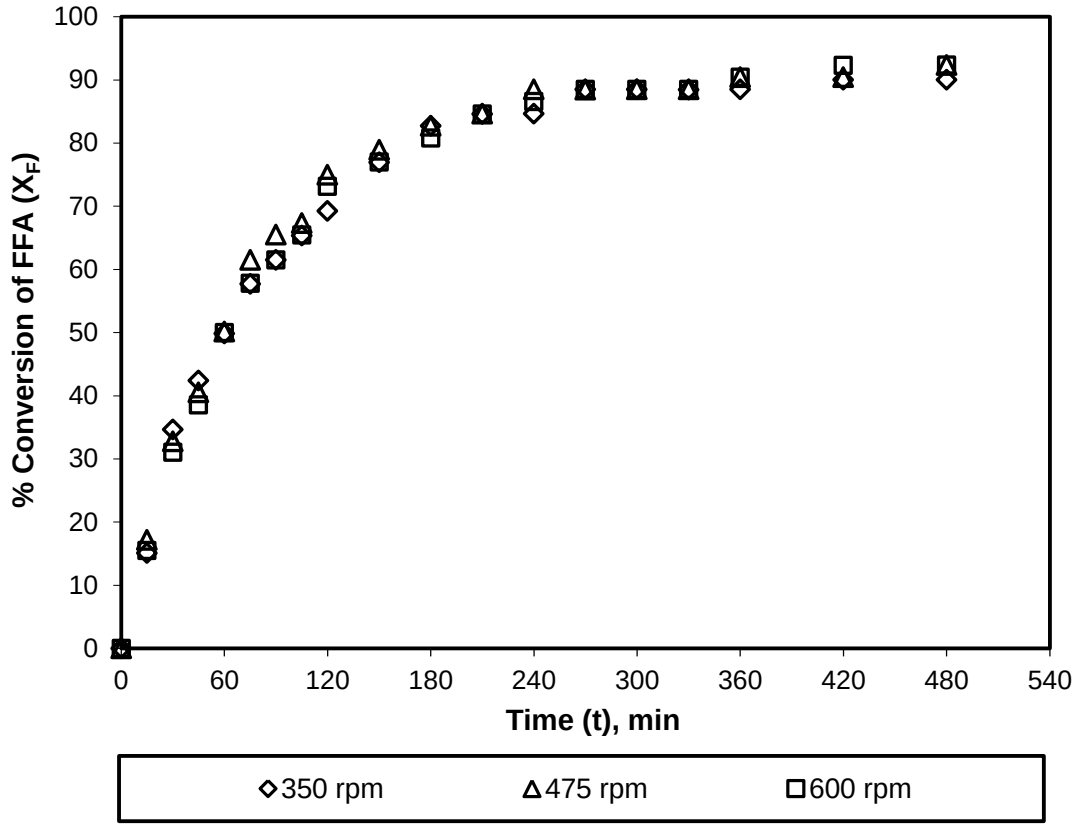

Figure 28.8 Effect of different stirring speed on the FFA conversion – External mass transfer resistance. Experimental conditions: catalyst: Purolite D5081; molar ratio (methanol:UCO): 6:1; catalyst loading:1.25% (w/w); reaction temperature: 60ºC**.

**Adapted with permission from Abidin et al., 2012, Industrial and Engineering Chemistry Research, 51: 14653–14664, American Chemical Society.

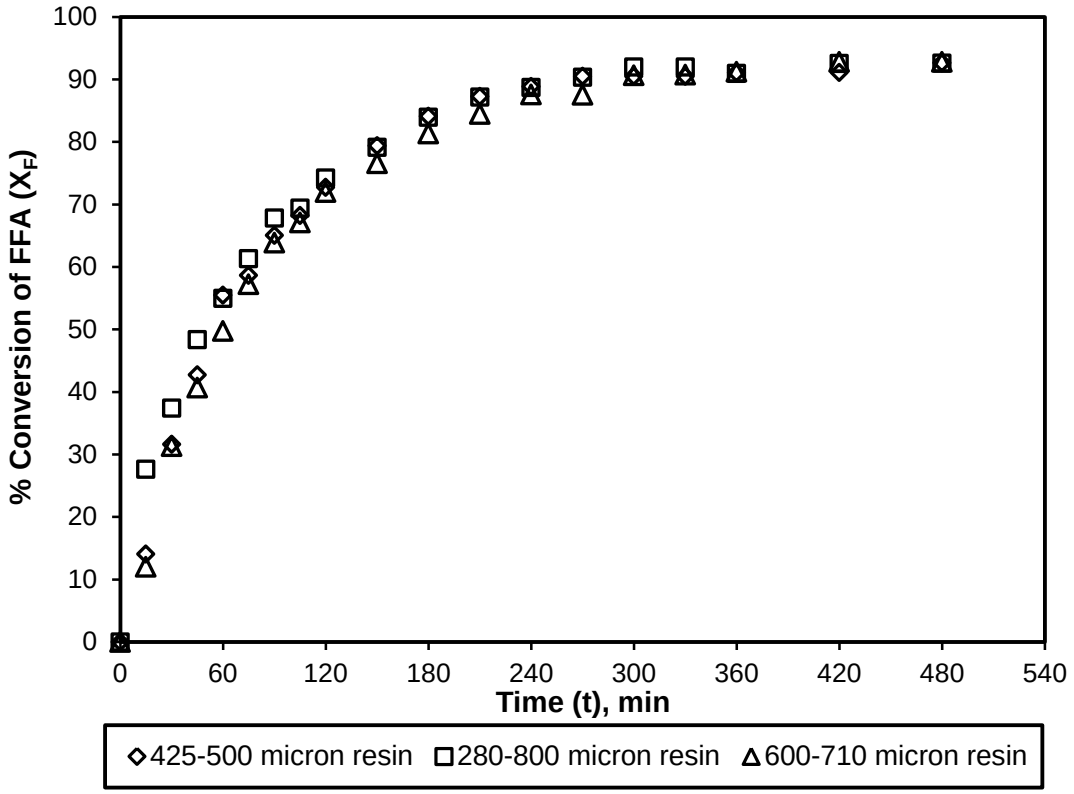

Figure 28.9 Effect of different resin size on the FFA conversion – Internal mass transfer resistance Experimental conditions: catalyst: Purolite D5081; stirring speed: 475 rpm; catalyst loading: 1.25% (w/w); reaction temperature: 60ºC; molar ratio (methanol:UCO): 6:1**.

**Adapted with permission from Abidin et al., 2012, Industrial and Engineering Chemistry Research, 51: 14653–14664, American Chemical Society.

28.3.2.3 *Effect of Catalyst Loading*

The effect of catalyst loading is shown in Figure 28.10. The reaction temperature was set at 60ºC with 6:1 methanol to UCO molar ratio, the reaction took approximately 8 h to reach equilibrium. The result shows that the conversion is greatly influenced by the amount of catalyst, especially at the early stage of the esterification reaction. This is attributed to the fact that as the catalyst loading increases, the number of active catalytic sites increases and a shorter time is required to reach equilibrium. Variation in catalyst loading also has an effect on the final conversion of FFA with the difference between the highest and the lowest catalyst loading of about 10%. At a low

catalyst concentration (<1% (w/w)), the difference in the conversion was significant. However, as catalyst loading was increased (≥ 1.25% (w/w)), the trends were less significant. This phenomenon indicates that as the percentage of resin increases, the conversion increases. However as the number of catalytic sites increases (≥ 1.25% (w/w) catalyst loading), the benefits are reduced as there are sufficient active catalytic sites in the reactant molecules to catalyse the reaction. In the case of the system investigated it was found that once the catalyst loading increased to 1.25% (w/w), there were sufficient catalyst sites for this particular reaction. As a result, 1.25% (w/w) loading was chosen as the optimum catalyst loading and was used for all further experimental work.

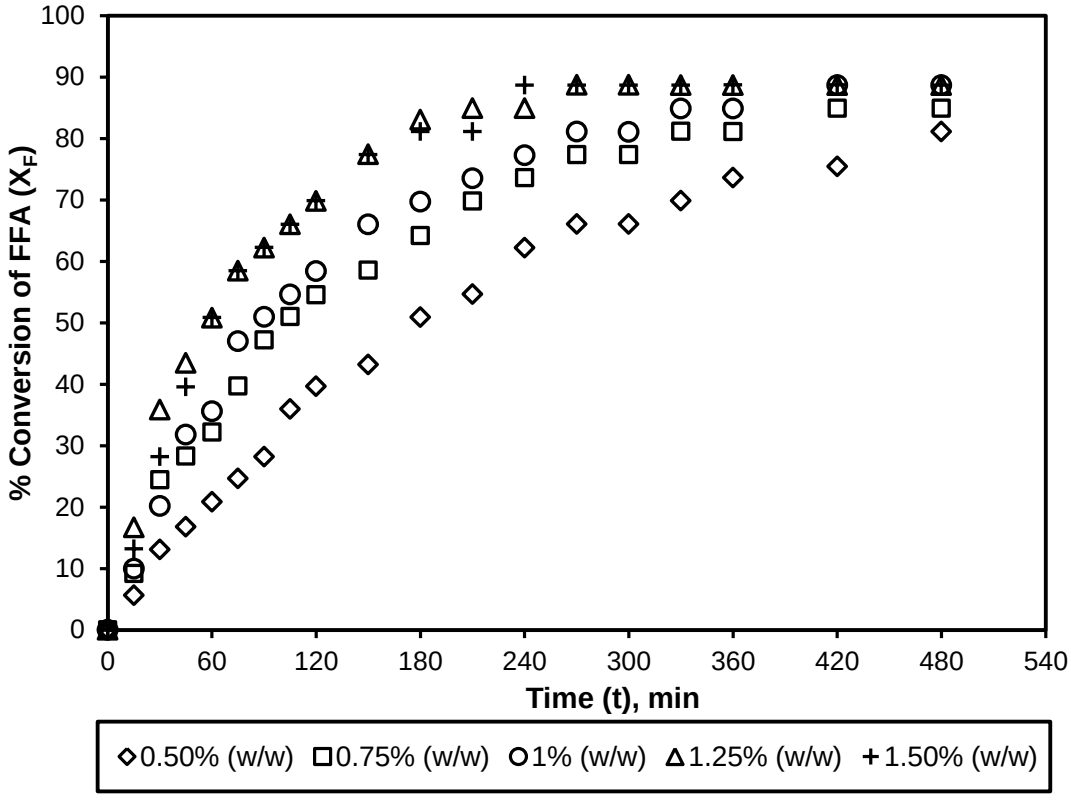

Figure 28.10 Effect of different catalyst loading on the FFA conversion. Experimental conditions: catalyst: Purolite D5081; stirring speed: 350 rpm; reaction temperature: 60ºC; molar ratio (methanol:UCO): 6:1**.

**Adapted with permission from Abidin et al., 2012, Industrial and Engineering Chemistry Research, 51: 14653–14664, American Chemical Society.

28.3.2.4 *Effect of Reaction Temperature*

Esterification was investigated at different temperatures (50, 55, 60, 62, 65°C) and the results are shown in Figure 28.11. It has been observed that increasing temperatures lead to reduction in the viscosity of UCO, which enhances the contact between the methanol and UCO leading to a higher conversion of FFA. The highest conversion was obtained at 65°C. A decrease in the volume of the reaction mixture was observed when the temperature reached the boiling point of methanol, 64.7°C. It was expected as there will be some changes to the system when this temperature is reached, with more methanol present in the headspace of the reactor as vapor. Liu *et al*. (2009) also claimed that beyond 65ºC, methanol started to vaporize rapidly, forming large number of bubbles to form foam and resulted in decrease in FFA conversion. Generally, in typical biodiesel reaction process, low temperature will result in lower conversion while higher temperatures lead to excessive methanol loss due to evaporation. After consideration of the safety issues, cost implications and the conversion trends for each temperature, the optimum reaction temperature was found to be 60°C.

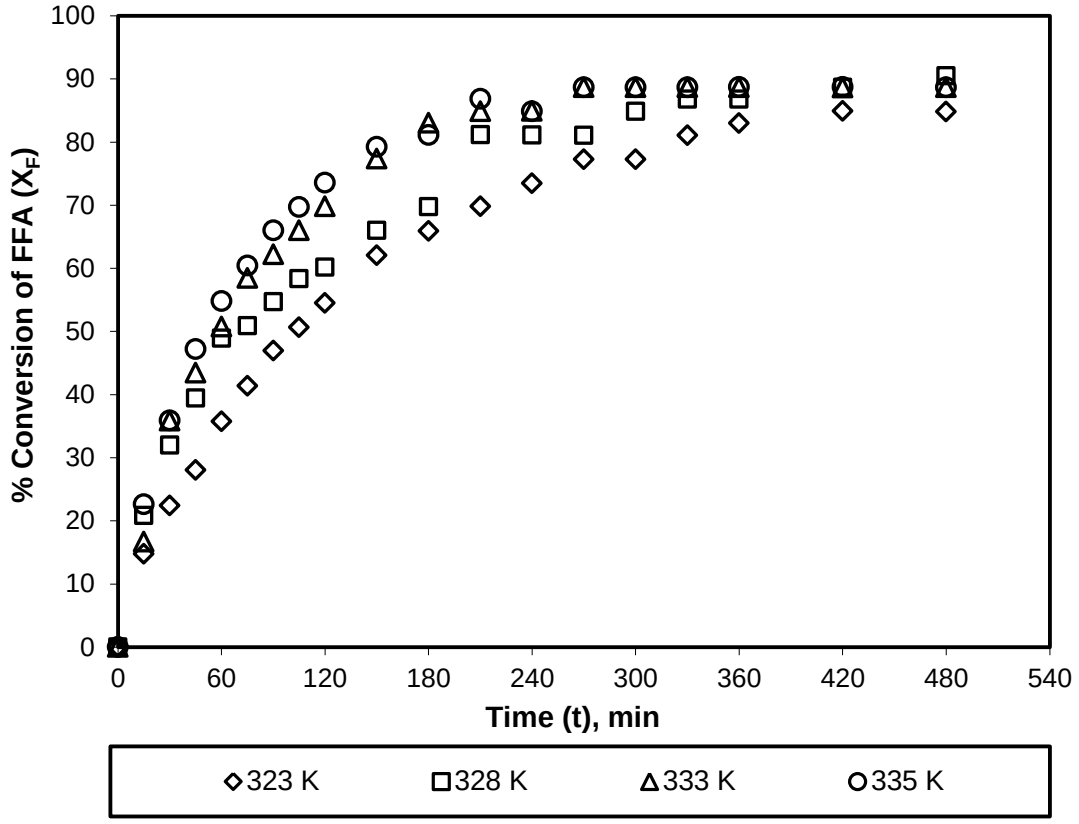

Figure 28.11 Effect of different reaction temperatures on FFA conversion. Experimental conditions: catalyst: Purolite D5081; stirring speed: 350 rpm; catalyst loading: 1.25% (w/w); molar ratio (methanol:UCO): 6:1**.

**Adapted with permission from Abidin et al., 2012, Industrial and Engineering Chemistry Research, 51: 14653–14664, American Chemical Society.

28.3.2.5 *Effect of Methanol to UCO Molar Ratio*

Figure 28.12 shows the effect of methanol to UCO molar ratio on the conversion of FFA. The reaction temperature was set at 60ºC, at 350 rpm stirrer speed with 8 h reaction time. The molar ratios were calculated based on the molecular mass of average fatty acid composition. From Figure 28.12 it can be seen that the conversion increased slightly with an increase in methanol to UCO molar ratio. However, the conversion differences between the molar ratios were less noticeable, giving about 2% increments in conversion as the molar ratio increases. In comparison, a ratio of 4:1 has a comparably lower initial conversion as compared to the other

three molar ratios. This will be due to insufficient methanol in the mixture to force the reaction, leading to longer reaction time to reach equilibrium. The reaction time can be shortened using a higher methanol to UCO molar ratio, however the costs will be higher due to higher methanol recovery requirements. A high molar ratio also leads to difficulties in the separation process, and thus hinders separation by gravity (Encinar et al., 2007). Furthermore, this situation i.e. high molar ratio could also increase the solubility of glycerine, and thus reduces the yield of FAME as glycerol remains in the pre-treated UCO phase. Excess methanol also could drive the combination of methyl ester and glycerine to monoglycerides, which increases the viscosity of the reaction mixture (Liu et al., 2009). Taking into account the safety issues and the capital and operating costs, a molar ratio of 6:1 (methanol: UCO) was chosen as the optimum molar ratio for the esterification reaction.

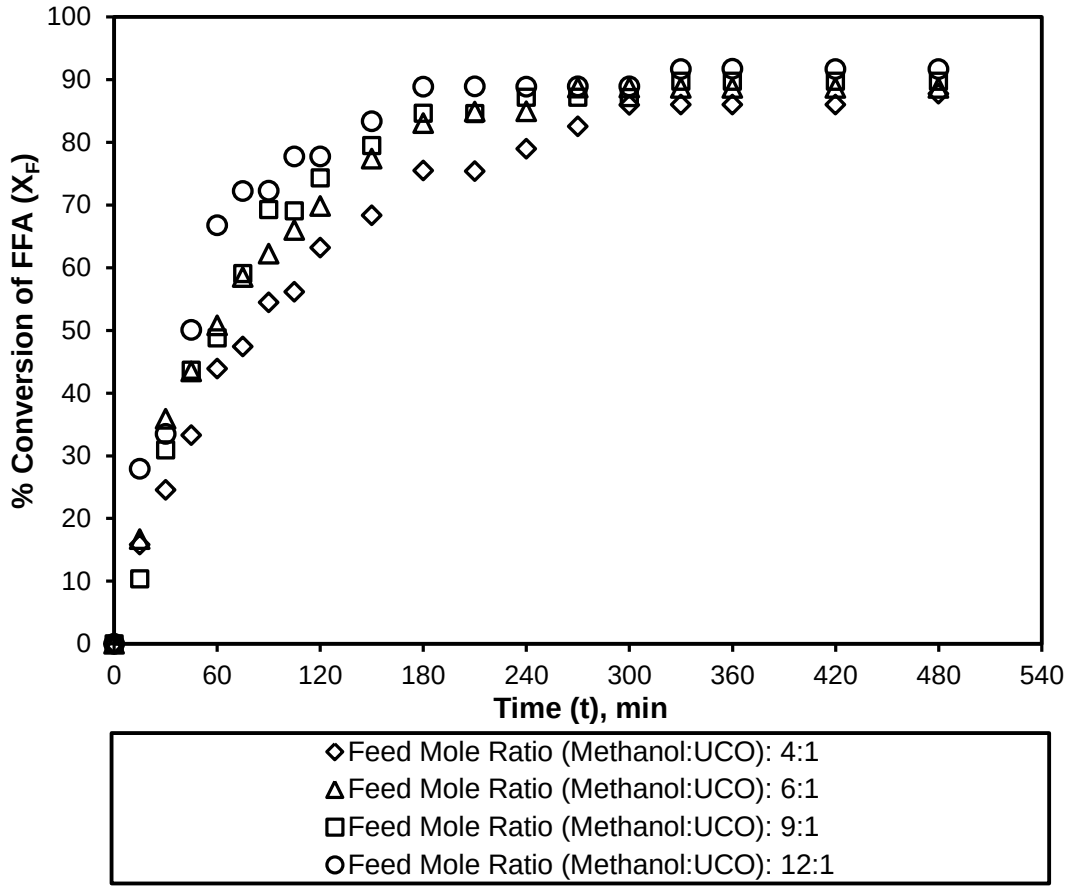

Figure 28.12 Effect of different molar ratio (methanol:UCO) on the FFA conversion. Experimental conditions: catalyst: Purolite D5081; catalyst loading: 1.25% (w/w); stirring speed: 350 rpm; reaction temperature: 60ºC**.

**Adapted with permission from Abidin et al., 2012, Industrial and Engineering Chemistry Research, 51: 14653–14664, American Chemical Society.

28.3.3 Transesterification Reaction

28.3.3.1 *Catalyst Screening Study*

The transesterification of biodiesel using different types of heterogeneous catalysts has been investigated to select the best catalyst for further optimisation work. There are two groups of catalysts involved in this work, which are the cation exchange resins (Purolite CT-122, Purolite CT-169, Purolite CT-175, Purolite CT-275, Purolite D5081) and anion exchange resin (Diaion PA306s) respectively. All catalysts were tested under the same reaction conditions, 1.5% (w/w)

of catalyst loading, 333 K reaction temperature, 18:1 methanol to P-UCO feed mole ratio and 350 rpm impeller stirring speed. The results are collected in Figure 28.13. After 8 h of reaction, the conversion of triglycerides was ca. 50% using Diaion PA306s catalyst, ca. 10% using Purolite CT-275 and ca. 7% using Purolite CT-122 and Purolite CT175. For Purolite D5081 catalyst, there was no measureable formation of FAME. Of all the catalysts investigated, Diaion PA306s gave the highest triglyceride conversion of ca. 50%.

From the results obtained, it was found that the specific surface area of the catalyst did not give any significant impact to the conversion of triglycerides. It was proven by having negligible triglycerides conversion when Purolite D5081, a catalyst with the highest specific surface area were used as the catalyst. The level of crosslinking also gives fluctuate performances where a low crosslinked resin Diaion PA306s gives the highest triglycerides conversion (ca. 50%) whereas the other low crosslinked catalyst, Purolite CT-122 was only able to give ca. 7% of triglycerides conversion. In contrast, Purolite CT-275, which has a high degree of cross-linking gives a slightly higher triglycerides conversion (ca. 10%) as compared to Purolite CT-122.

A huge difference in catalytic performance was observed between Diaion PA306s and the other catalysts and it was expected to be closely related to the acidity and basicity of the catalysts. In this case, Diaion PA306s was classified as a strongly basic anion exchange resin, whilst the rest of the catalysts are categorised as strongly acidic resins. Few researchers (Mazzotti *et al.* (1997) and Shibasaki-Kitakawa *et al.* (2007)) have also reported that the adsorption strength of the alcohol on the anion exchange resin was much higher as compared to cation exchange resins, which results in higher activity for anion exchange resin as compared to cation exchange resin. Therefore, it was concluded that the basicity of the catalyst is responsible for its transesterification activity and not specific surface area, particle size distribution, average pore

diameter or the crosslinking level. Since Diaion PA306s showed the best catalytic performance, it was used for the subsequent transesterification reactions.

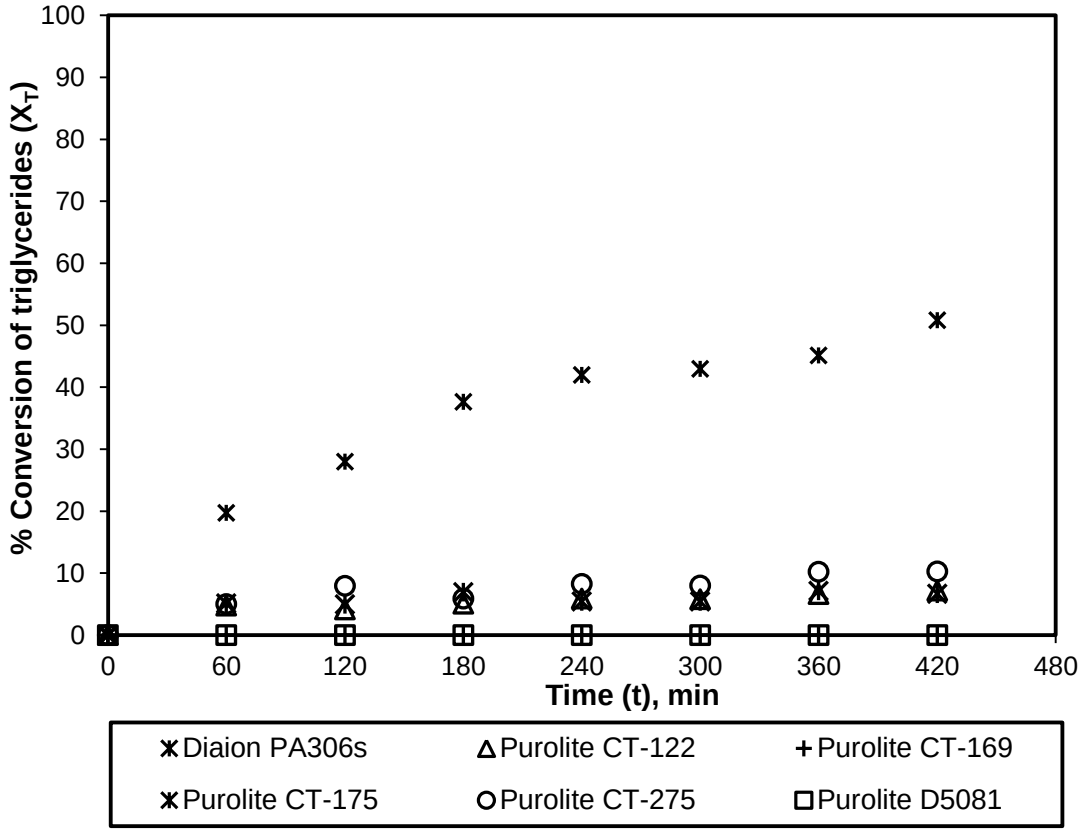

Figure 28.13 Effect of different types of catalysts on triglycerides conversion. Experimental condition: Stirring speed: 350 rpm, catalyst loading: 1.5% (w/w); reaction temperature: 333 K; feed mole ratio (methanol:P-UCO): 18:1.

28.3.3.2 *Investigation on the Effect of Mass Transfer Resistances in Transesterification Reaction*

There are two types of mass transfer resistances involved in ion exchange catalysis, the external mass resistance and internal mass transfer resistance. The external mass transfer resistance, which takes place across the solid-liquid interface, was evaluated using different stirring speeds under the same reaction conditions. Three different agitation speeds were used, 300, 350 and 450

rpm and the result is shown in Figure 28.14. It was found that the stirring speed gives a negligible impact on triglycerides conversion and therefore it was confirmed that the external mass transfer resistance has negligible effect on the transesterification reaction. The internal mass transfer resistance associated with the differences in particle size of the catalysts can be studied by measuring reaction rates for different average catalyst particle sizes. In this case, absence of internal mass transfer resistance could not be verified because the catalyst was supplied in wet form in the swelling condition. This type of catalyst (anion exchange resin) cannot be heated to more than 333 K, otherwise it affects the stability of the catalyst. As the moisture content cannot be totally removed below 333 K, separation by a sieving will not represent the actual size of catalyst particle. Therefore, PA306s resin was used as received, without sieving for all transesterification reaction.

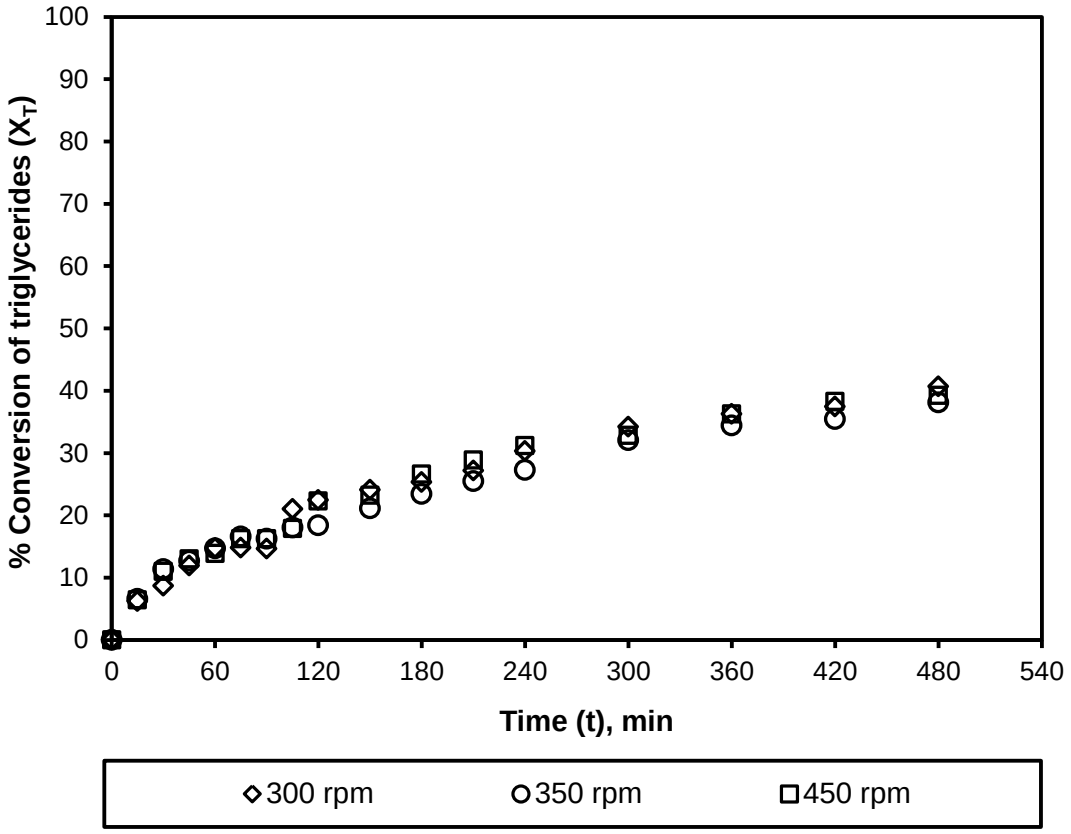

Figure 28.14 Effect of stirring speed on triglycerides conversion - External mass transfer resistance. Experimental conditions: Catalyst: Diaion PA306s; catalyst loading: 1.5% (w/w); reaction temperature: 323 K; feed mole ratio (methanol:P-UCO): 18:1.

28.3.3.3 *Effect of Catalyst Loading*

The effect of catalyst concentration on triglycerides conversion was investigated using different catalyst loadings, 1.5% (w/w), 3% (w/w), 4.5% (w/w), 5.5% (w/w), 9% (w/w) and 10% (w/w). Figure 28.15 shows the effect of catalyst loading on the conversion of triglycerides. The reaction temperature was set at 323 K with 18:1 methanol to P-UCO feed mole ratio and 350 rpm stirring speed. As observed from Figure 28.15, increasing the catalyst concentration was found to increase triglycerides conversion. This behaviour was expected since with an increase in the number of active catalytic sites, triglycerides conversion increases. As the reaction proceeds, the changes in triglycerides conversion become less significant, indicating that the system is

approaching equilibrium. Based on the observation for 9% (w/w) and 10% (w/w) catalyst loading, it could be concluded that a further increase in catalyst concentration would cause negligible increase in the conversion of triglycerides (ca. 64% to 65%). Furthermore, higher catalyst dosage increases the viscosity of the reaction mixtures that increases the mass transfer resistance in the multiphase system. Therefore, using a very high amount of catalyst is unnecessary for this reaction. For all further transesterification study, 9% (w/w) was chosen as the optimum catalyst loading.

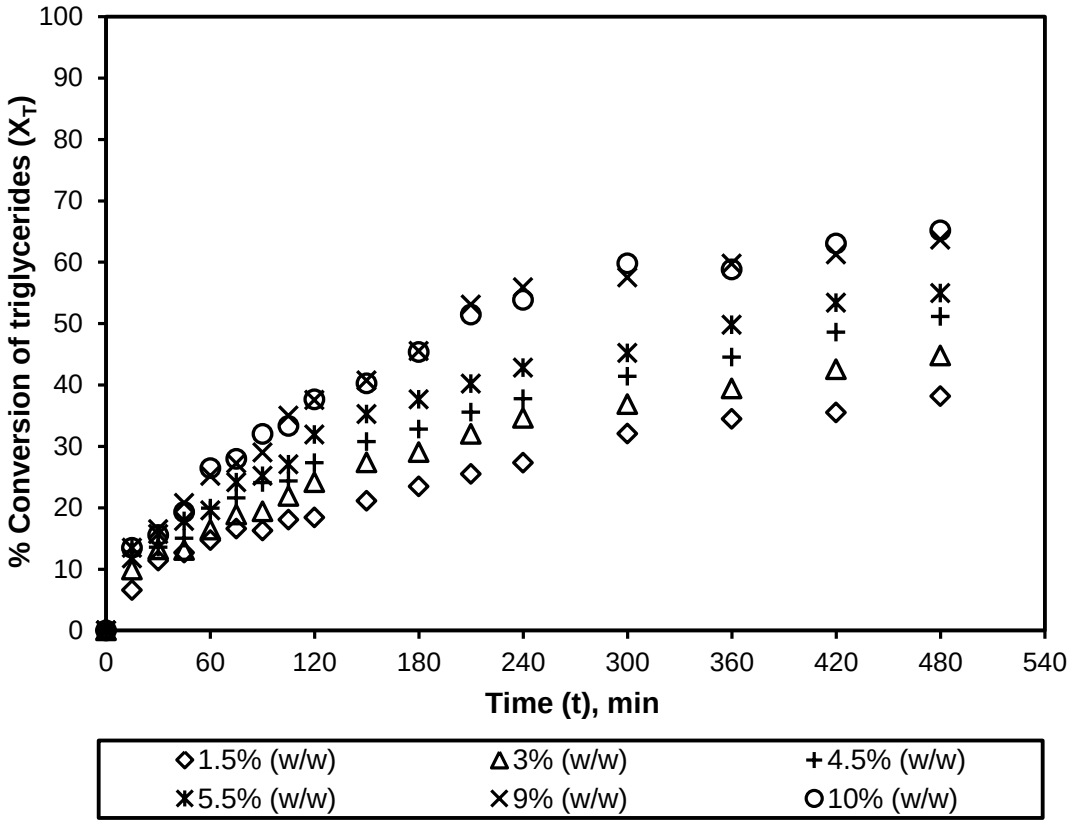

Figure 28.15 Effect of catalyst loading on triglycerides conversion. Experimental conditions: Catalyst: Diaion PA306s; stirring speed: 350 rpm; reaction temperature: 323 K; feed mole ratio (methanol:P-UCO): 18:1.

28.3.3.4 *Effect of Reaction Temperature*

Figure 28.16 shows the plot of triglycerides conversion over time with the temperature ranging from 313 to 333 K. From the figure, triglycerides conversion was found to increase with an increase in reaction temperature. After 8 h of reaction, the final conversion of triglycerides at 313, 325 and 328 K was approximately 50%, 64% and 75%, respectively. Theoretically, an increase in reaction temperature leads to a reduction in the viscosity of triglycerides, which enhances the contact between methanol and triglycerides. From Figure 28.16, it was also observed that triglycerides conversion for the 328 and 333 K reaction temperatures are similar although the time for the conversion to reach steady state was faster for 333 K. As the final conversion for 325 and 328 K was approximately the same with ca. 75% conversion, an increase in temperature will only increase the operating cost. Therefore, 325 K was chosen as the optimum reaction temperature and proposed for further transesterification reactions.

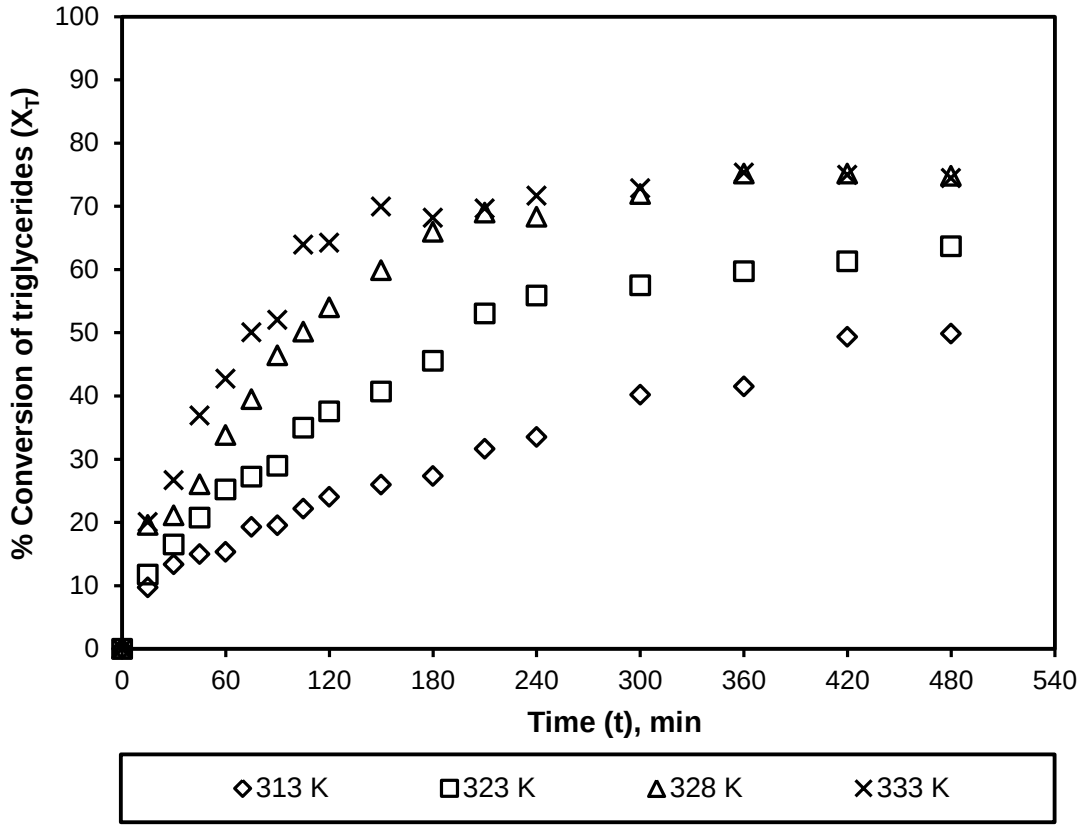

Figure 28.16 Effect of reaction temperature on triglycerides conversion. Experimental conditions: Catalyst: Diaion PA306s; stirring speed: 350 rpm; catalyst loading: 9% (w/w); feed mole ratio (methanol:P-UCO): 18:1.

28.3.3.5 *Effect of Methanol to P-UCO Feed Mole Ratio*

Stoichiometrically, the methanolysis of triglycerides requires three moles of methanol per mole of triglyceride to yield three moles of FAME and one mole of glycerine. Given that the transesterification is a reversible reaction, excess methanol should help the conversion of triglycerides. The molar mass of UCO was determined to be 871.82 g mol^{-1} and this was used to calculate the feed mole ratio of methanol to P-UCO. Figure 28.17 shows the effect of feed mole ratio of methanol to P-UCO on the conversion of triglycerides. As observed from Figure 28.17, the conversion of triglycerides increased with an increase in methanol to P-UCO feed mole ratio

from 6:1 to 18:1. The conversion of triglycerides using 6:1, 12:1 and 18:1 methanol to P-UCO feed mole ratio at 8 h are 63%, 69% and 75%, respectively. From Figure 28.17, it can be seen that a further increase in feed mole ratio of methanol to P-UCO from 18:1 to 24:1 did not result in an increase in conversion of triglycerides and the final triglycerides conversion for both feed mole ratios were approximately same, i.e. 75%. A significantly high feed mole ratio is not preferable in biodiesel production because it makes the separation process difficult and higher consumption of methanol also requires larger unit operations including reactors, separation column and methanol recovery equipment that will increase the overall cost of the process. An optimum operating ratio should be selected on the basis of overall economics and equilibrium conversion and therefore, a feed mole ratio of 18:1 methanol to P-UCO was selected as the optimum ratio and used for further transesterification reaction.

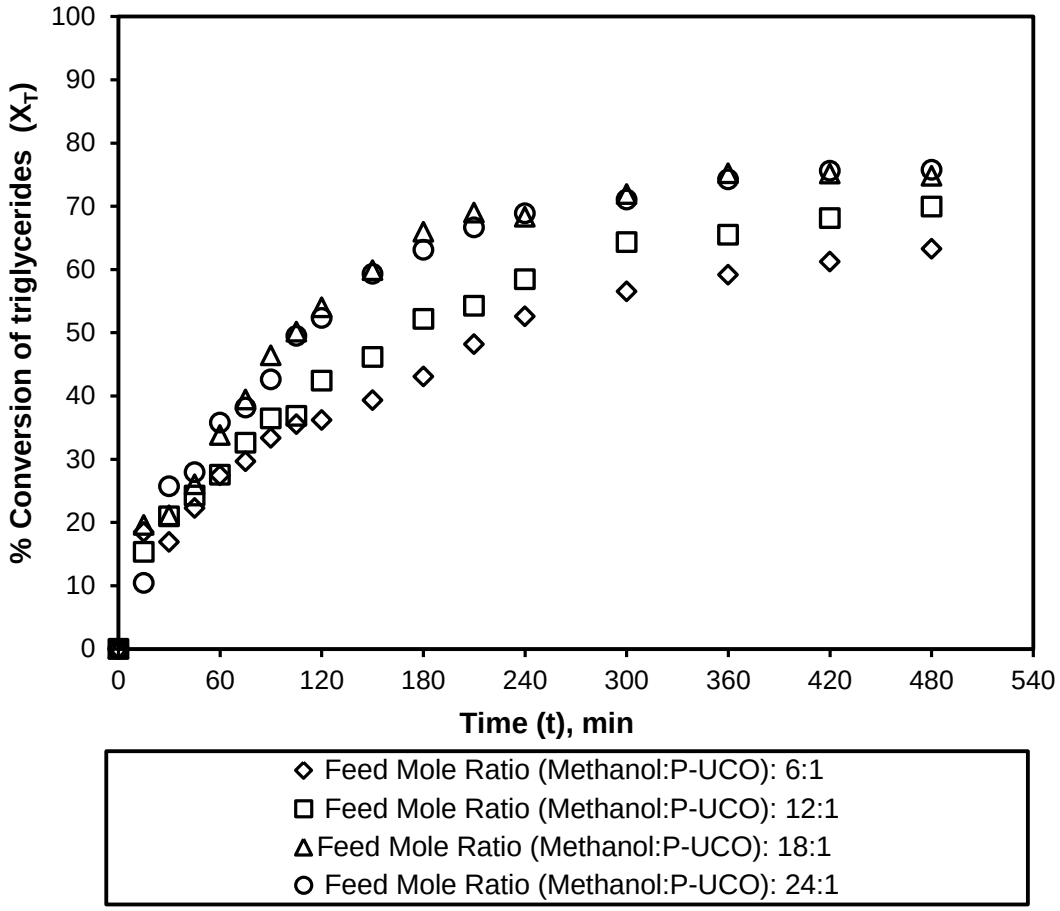

Figure 28.17 Effect of feed mole ratio (methanol:P-UCO) on triglycerides conversion. Experimental conditions: Catalyst: Diaion PA306s; stirring speed: 350 rpm; catalyst loading: 9% (w/w); reaction temperature: 328 K.

28.3.4 Catalyst Reusability Study

28.3.4.1 *Reusability study on the spent esterification catalyst*

A series of reactions, using the same batch of Purolite D5081 catalyst, were carried out at optimum process conditions, i.e. 1.25% (w/w) catalyst loading, 333 K reaction temperature, 6:1 methanol to UCO feed mole ratio, and 475 rpm stirring speed, to determine the catalyst life span. The results are shown in Figure 28.18 and from this data it can be seen that the conversion decreased by approximately 8-10% per cycle (e.g. fresh catalyst gives ~92% conversion, the first cycle gives ~84% conversion and the second cycle gives ~73% conversion). Potential reasons for

the loss of activity include contamination of the external or internal surface of the catalyst and sulphur leaching.

SEM analysis was used to investigate the effect of cleaning regimes on the surface of the ion exchange resin catalysts. Purolite D5081 was cleaned by placing the catalyst in a flask of methanol which was subsequently placed in an ultrasonic bath and the method is detailed in Section 1.2.6. To determine the effect of ultrasonication, Purolite D5082 was cleaned using methanol but without ultrasonication. A series of SEM images are shown in Figure 28.19, which show the comparison of fresh and used catalyst (after the first run) as well as comparing the effect of cleaning regimes. Figures 28.19(a) and 28.19(b) show a sample of Purolite D5081 before and after esterification and it can be seen that there is no trace of UCO on the surface of the used catalyst in Figure 28.19(b). Figures 28.19(c) and 28.19(d) show a sample of Purolite D5082 before and after esterification and in this case it can be seen that there is UCO present on the surface of the catalyst, indicating incomplete washing of the catalyst. This observation fits with the results of the elemental analysis for used D5082 (Table 28.4) which shows there is a slight increase in residual carbon. On this basis it was decided that ultrasonication was needed as part of the cleaning process in order to ensure UCO was removed from the surface of the catalyst.

Contamination of the internal surface of the catalyst could possibly result from the resin pore blockage, either by the presence of metal ions in the UCO or the blockage by the UCO residue itself. An energy-dispersive X-ray spectroscopy (EDX) analysis of fresh and used Purolite D5081 catalysts has been conducted and trace amount of metal was found on the catalyst. The amount of sodium and iron content was very similar for both fresh and used Purolite D5081 catalysts (~0.20% and ~0.15%). In the used Purolite D5081 catalyst, trace amount of calcium

ions was found (approximately 0.012-0.10%). Given that only trace amount of metal was found on the surface of the catalyst, it has been concluded that the metal ion impurities in UCO do not contribute to the deactivation of Purolite D5081 catalyst.

It was found that the mass of catalyst increased slightly after each reaction cycle and it has been assumed that this was due to the presence of triglycerides, proteins, trace amount of phospholipids and other impurities in UCO that could potentially foul Purolite D5081 catalyst. The Brunauer-Emmett-Teller (BET) analysis showed that Purolite D5081 resin has highest total pore volume of 0.47 cm^3/g, which was slightly higher than other conventional ion exchange resins. This means it is possible for the triglycerides, proteins and trace amount of phospholipids molecules to be retained within the resin catalyst and may contribute to pore blockage. This may also reduce the accessibility of the active catalyst sites and may lead to higher internal mass transfer resistance and finally contribute to decreasing catalytic activity.

Sulphur leaching occurs due to the detachment of sulphonic acid group from the polymer matrix. Water is one of the products formed during the esterification reaction and in theory it could hydrolyse sulphonic acid groups to form homogenous sulphuric acid. An elemental analysis was carried out to determine the level of sulphur within various resin samples and the results are shown in Table 28.4. Fresh D5081 resin had a sulphur content of 4.1%, and after the first reaction cycle this decreased by nearly 20% to 3.3%. Ion exchange capacity results in Table 28.5 show a decrease of acid capacity for fresh and used catalyst of approximately 13%. This indicates that sulphur leaching contributes to the reduction in catalytic activity of Purolite D5081 catalyst.

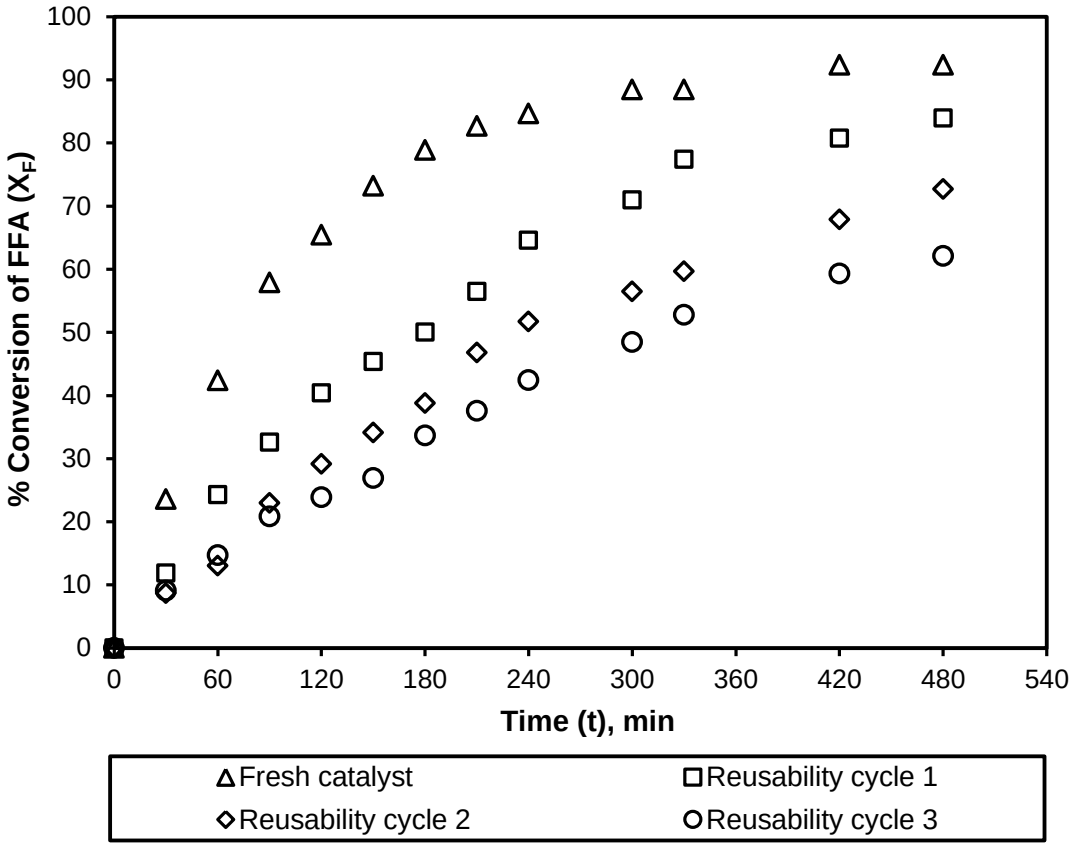

Figure 28.18 Reusability study on Purolite D5081 ion exchange resins. Experimental conditions: catalyst: Purolite D5081; stirring speed: 475 rpm; catalyst loading: 1.25% (w/w); reaction temperature: 60ºC; molar ratio (methanol:UCO): 6:1**.

**Adapted with permission from Abidin et al., 2012, Industrial and Engineering Chemistry Research, 51: 14653–14664, American Chemical Society.

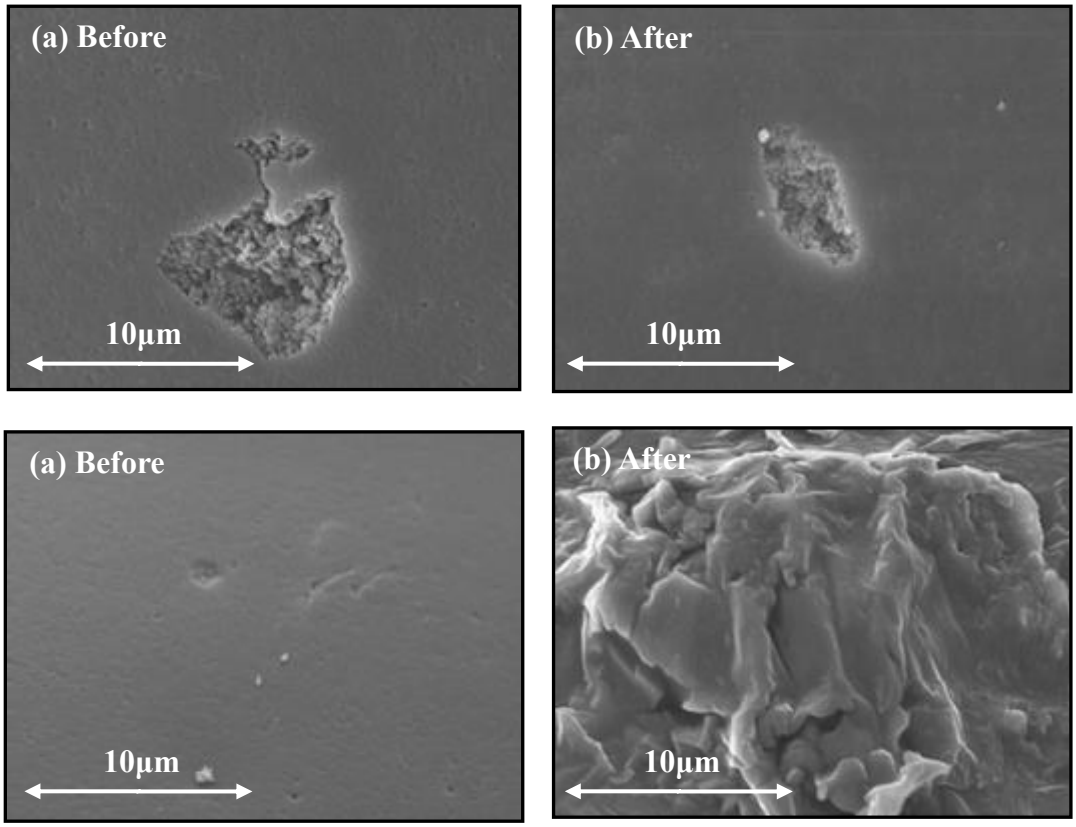

Figure 28.19 SEM analysis of Purolite catalysts taken at 5000x magnification: Figure 28.19(a) and Figure 28.19(b) is Purolite D5081 before and after esterification process and Figure 28.19(c) and Figure 28.19(d) is Purolite D5082 before and after esterification process**.

**Adapted with permission from Abidin et al., 2012, Industrial and Engineering Chemistry Research, 51: 14653–14664, American Chemical Society.

To further investigate the leaching of homogeneous species in the reaction mixture and UCO blockage within the resin pores, several sets of experiments have been carried out. The experimental work and the process flow diagram have been detailed in section 28.2.6 and Figure 28.4, respectively. Figure 28.20 shows the conversion of FFA during the uncatalysed reaction between the treated-methanol solution and UCO and this result clearly shows there was a significant FFA conversion for the first cycle of homogeneous contribution study. This confirms the occurrence of sulphonic acid group leaching, believed to be due to the detachment of sulphonic acid group from the catalyst surface, followed by the hydrolysis of sulphonic acid

species with water to form homogeneous species. Data for the second cycle shows after the first homogenous contribution cycle that conversion is very low indicating that there is no further leaching of the sulphonic acid group into methanol in subsequent cycles.

In addition, the catalyst deactivation has also been investigated using the catalyst that was previously filtered from the methanol solution. The results were summarized in Figure 28.21. From the figure, it could be seen that the conversion for the second cycle was slightly lower compared to the first cycle. This was solely due to the blockage of large molecules of UCO molecules as the data from Figure 28.20 shows that the leaching of sulphonic acid was negligible during the second cycle of the reaction.

Figure 28.22 shows the comparison between the reusability study and methanol treated catalyst study. The difference in FFA conversion between the fresh catalyst and first methanol treated catalyst cycle is believed to be due to leaching of sulphonic acid groups. This is because both experiments were conducted at the same experimental parameters, the only difference was the condition of the catalyst, where the former experiment used fresh catalyst and the latter one used methanol-treated-catalyst. This finding was verified using the homogeneous contribution study shown in Figure 28.20.

On the other hand, the first cycle of methanol treated catalyst study gives a conversion close to the first cycle from the reusability study. For the former experiment, the resin itself was not introduced to any UCO mixture, so there was no possibility of any triglyceride blockage during the reaction and this means the conversion was slightly higher. So, it could be inferred that the 6% reduction in conversion was solely due to blockage of large UCO molecules in the catalysts' pores. The same trend was observed during the second cycle for both cases where the calculated conversion difference was about the same. Therefore, it could be concluded that the reduction of

FFA conversion in subsequent cycles (either for the reusability study or the methanol treated catalyst study) is largely due to the progressive blockage of the large triglycerides molecules in the pores of the resin, since there is a steady reduction in the FFA conversion for each cycle. Furthermore, the possibility of sulphonic acid groups leaching throughout the process was small. When both conditions (reusability study and methanol treated catalyst study) were evaluated individually, both of them showed sulphur leaching and pore blockage simultaneously, and show a reduction in FFA conversion with increasing cycle number.

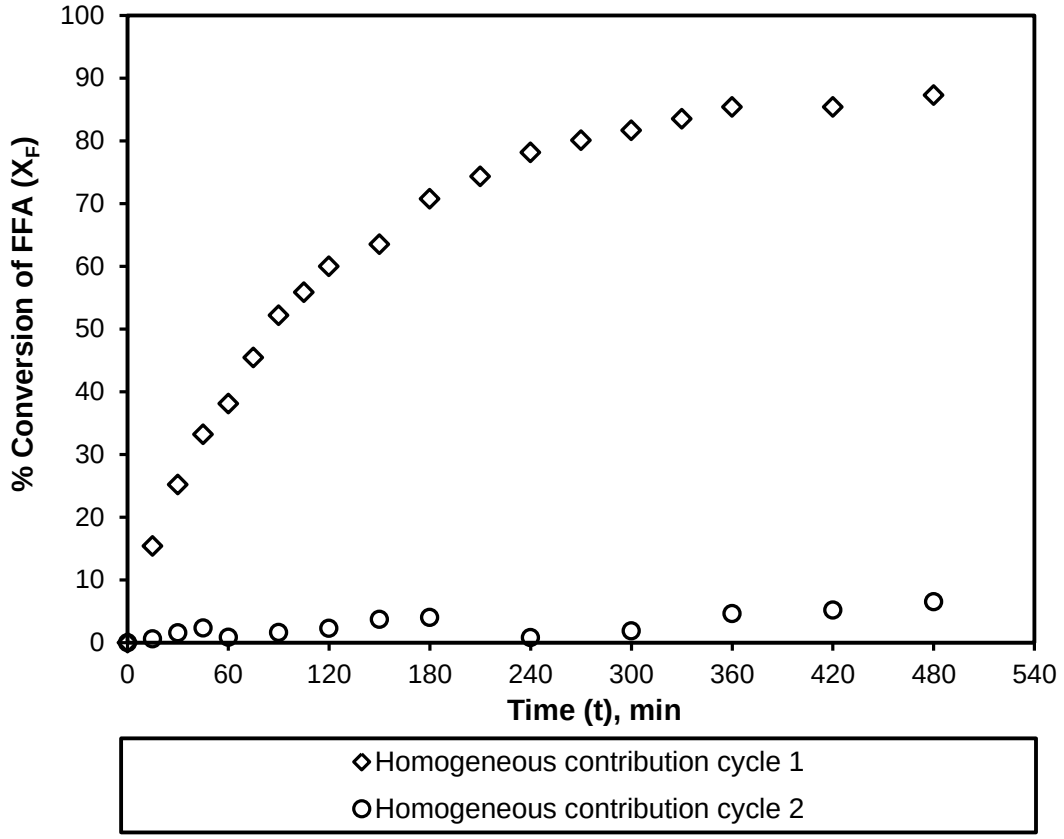

Figure 28.20 Study on the homogeneous contribution of Purolite D5081 ion exchange resins. Experimental conditions: catalyst: Purolite D5081; stirring speed: 475 rpm; reaction temperature: 60ºC**.

**Adapted with permission from Abidin et al., 2012, Industrial and Engineering Chemistry Research, 51: 14653–14664, American Chemical Society.

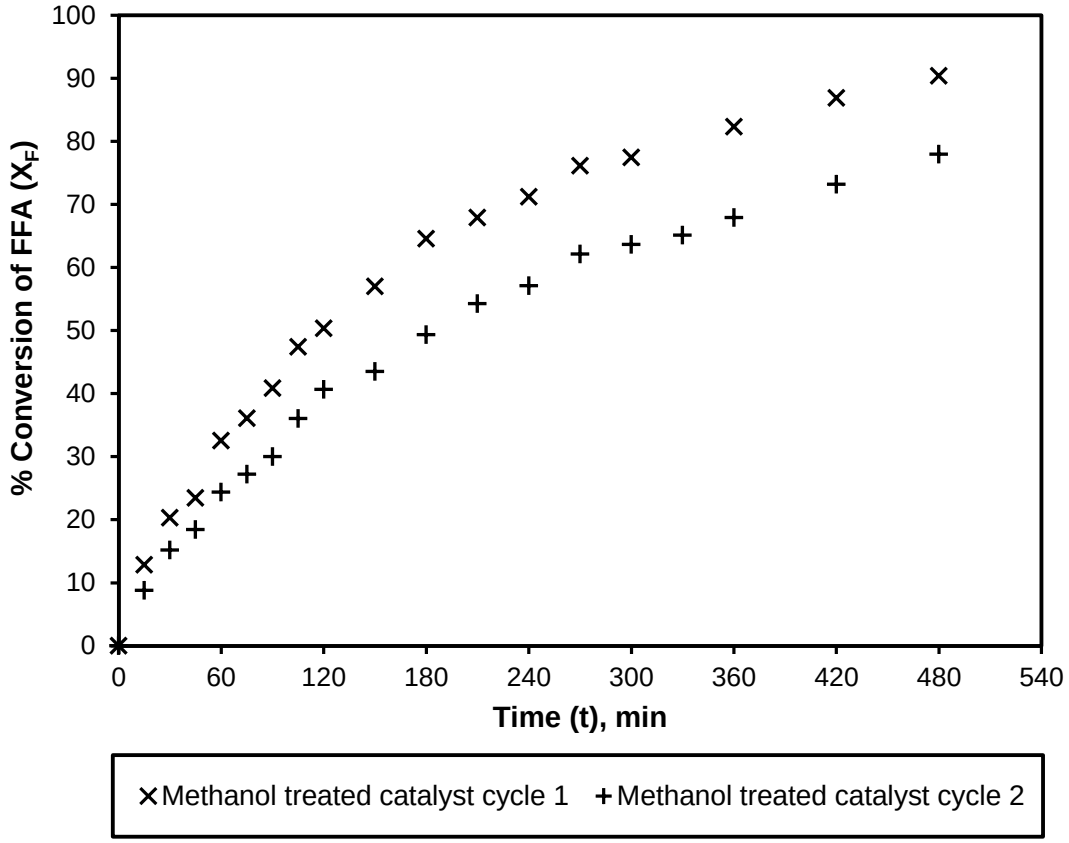

Figure 28.21 Study on the methanol treated catalyst deactivation. Experimental conditions: catalyst: Purolite D5081; catalyst loading; 1.25% (w/w), stirring speed: 475 rpm; reaction temperature 60ºC; molar ratio (methanol:UCO): 6:1**.

**Adapted with permission from Abidin et al., 2012, Industrial and Engineering Chemistry Research, 51: 14653–14664, American Chemical Society.

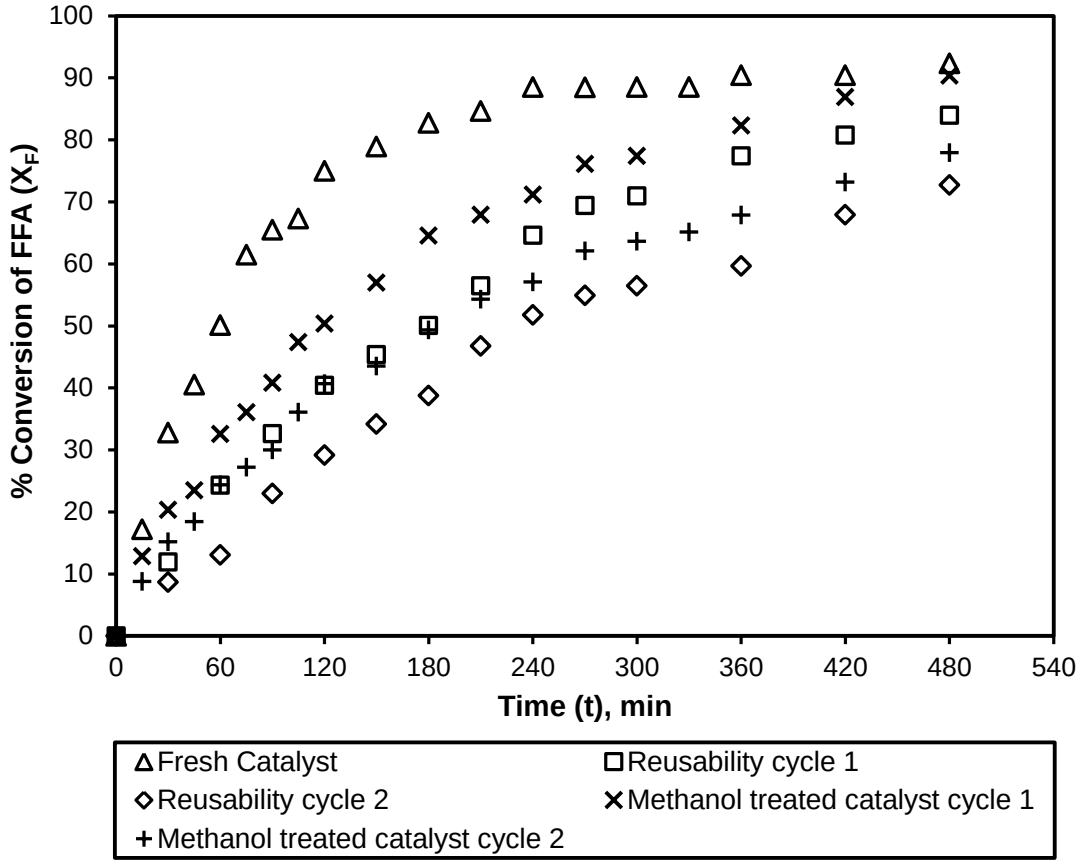

Figure 28.22 Comparison between the reusability study and the methanol treated catalyst study. Experimental conditions: catalyst: Purolite D5081; stirring speed: 475 rpm; catalyst loading: 1.25% (w/w); reaction temperature: 60ºC; molar ratio (methanol:UCO): 6:1**.

**Adapted with permission from Abidin et al., 2012, Industrial and Engineering Chemistry Research, 51: 14653–14664, American Chemical Society.

28.3.4.2 *Reusability study on the spent transesterification catalyst*

Reusability of the catalyst is an important step as it reduces the cost of biodiesel production. During the preparation of used catalyst, the displacement of fatty acid ion with acetate ion was investigated using acetic acid concentrations of 17.5 M and 1 M, respectively. Two analyses (FEG-SEM and elemental analysis) were conducted before the displacement process was finalised.

The FEG-SEM analysis was carried out to observe any changes on the surface of the catalysts after being treated with acetic acid. Figure 28.23 compares the FEG-SEM analysis for (a) fresh Diaion PA306s, (b) used Diaion PA306s (1 M acetic acid treatment) and (c) used Diaion PA306s (17.5 M acetic acid treatment) catalysts captured at 500× magnification.

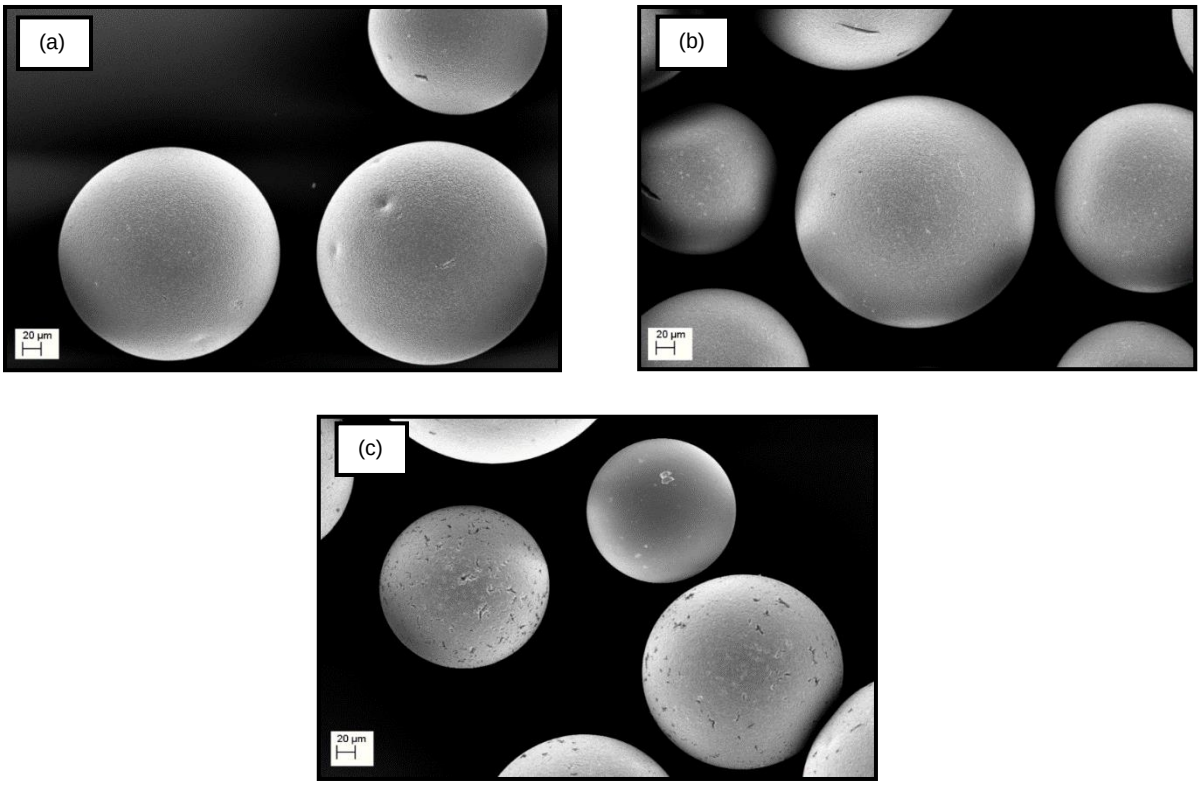

Figure 28.23 The FEG-SEM images of Diaion PA306s catalysts, taken at 500x magnification: (a) Fresh Diaion PA306s, (b) used Diaion PA306s (1 M acetic acid treatment) and (c) used Diaion PA306s (17.5 M acetic acid treatment).

From Figure 28.23, it can be seen that the surface morphology of fresh and used Diaion PA306s (1 M of acetic acid treatment) catalysts appears as a smooth surface whereas a noticeable deterioration of the surface was found when Diaion PA306s catalyst was treated with 17.5 M acetic acid. This suggests that the concentration of acetic acid is too high. Table 28.6 shows the results of the elemental analysis. From Table 28.6, it can be seen that the used Diaion PA306s

catalysts treated with 17.5 and 1 M acetic acid resulted in a slightly lower carbon and hydrogen values as compared to the fresh Diaion PA306s. The reduction of carbon and hydrogen values in used Diaion PA306s catalyst treated with 17.5 M of acetic acid was also found to be slightly higher than the used Diaion PA306s catalyst treated with 1 M of acetic acid. This indicates that there are some changes or damage to the structure of Diaion PA306s catalyst when higher acetic acid concentration was used and this could contribute to a loss in catalytic activity. Therefore, acid displacement using 1 M acetic acid solution was selected and further displacement process, as mentioned in section 1.2.6.

Table 28.6 Elemental analysis of fresh and used Diaion PA306s

Catalysts	**Elemental Analysis**			
	%C	**%H**	**%N**	**%O***
Fresh Diaion PA306s	55.59	9.42	4.34	30.65
Used Diaion PA306s (1 M acetic acid)	55.44	9.20	4.31	31.05
Used Diaion PA306s (17.5 M acetic acid)	54.51	8.84	4.35	32.30

*Oxygen by difference

The reusability study was carried out under the optimum reaction conditions, 9% (w/w) catalyst loading, 328 K reaction temperature, 18:1 methanol to P-UCO feed mole ratio and 350 rpm stirring speed. The result of reusability study was compared with the optimum result obtained using fresh Diaion PA306s catalyst and shown in Figure 28.24. It was observed that the Diaion PA306s catalyst gave a similar conversion of triglycerides using fresh and used catalysts. The conversion of triglycerides for both catalysts after 8 h of reaction time was approximately 75%. It was concluded that the catalyst can be used several times without losing catalytic activity.

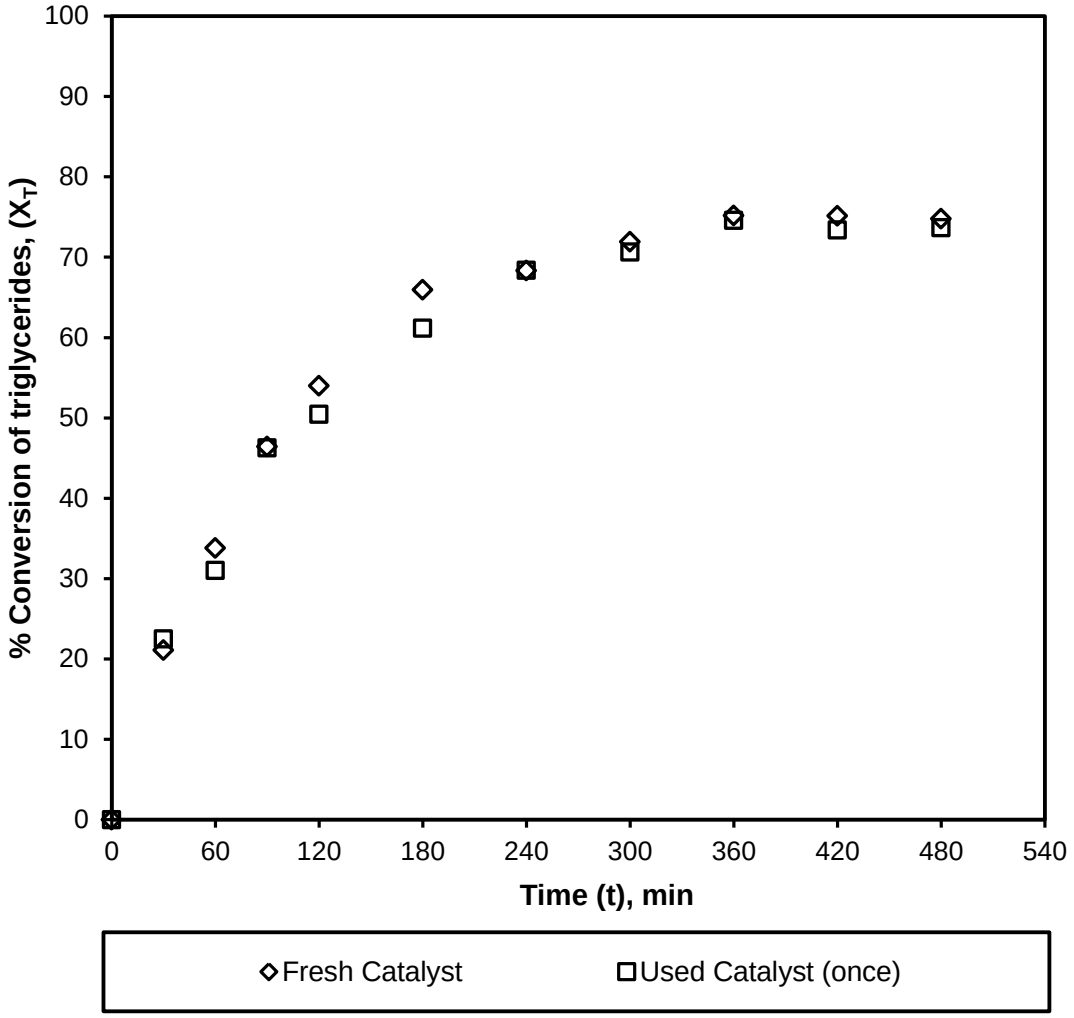

Figure 28.24 Effect of catalyst reusability on the conversion of triglycerides. Experimental conditions: Catalyst: Diaion PA306s; stirring speed: 350 rpm; catalyst loading: 9% (w/w); reaction temperature: 328 K; feed mole ratio (methanol:UCO): 18:1.

28.3.5 Separation and Purification Process

Once the transesterification reaction was completed, the reaction mixture was allowed to cool to room temperature. The reaction mixture was separated from the catalyst and transferred to a separating funnel. The reaction mixture was allowed to settle overnight to form FAME-rich phase and glycerine-rich phase layers. The layers were sequentially withdrawn from the separating funnel and introduced to the washing process. Two types of washing techniques were

examined, the conventional wet washing techniques using water and the dry washing techniques using Purolite PD206 as an adsorbent. Table 28.7 shows the purity of FAME using wet and dry washing and the results were compared with the unpurified biodiesel. Results in Table 28.7 show a similar percentage of FAME for all purified and unpurified samples. The dry washing treatment using PD 206 gave the highest percentage of FAME purity of ca. 75%. By having the advantage of being water-free, there is less production of wastewater; purified biodiesel from the dry washing treatment was selected for further testing.

Table 28.7 Purity of FAME using different treatment processes. (i) Ion exchange treatment, (ii) water treatment and (iii) unpurified biodiesel

Treatment Processes	**Purity of FAME, %**
Ion Exchange resin (PD 206) Treatment	75.4 ± 1
Water Treatment	72.3 ± 2
Unpurified biodiesel	71.6 ± 0.5

The purified biodiesel from the dry washing process was tested for monoglycerides, diglycerides, triglycerides and glycerine content. The same analyses were conducted on unpurified biodiesel and the results are presented in Table 28.8. It can be seen from Table 28.8 that biodiesel from the dry washing technique shows a lower percentage of glycerides and glycerine content as compared to the unpurified biodiesel. The finding contradicts with the findings by Shibasaki-Kitakawa *et al.* (2011) as they claimed that all the impurities such as the residual oil, FFA, water and dark brown pigment can be removed from the product by adsorption on Diaion PA306s catalyst.

Table 28.8 Analysis of monoglycerides, diglycerides, triglycerides and glycerine content (total and free glycerine)

Component	Ion Exchange Resin (PD 206) Treatment% (m/m)	Unpurified Biodiesel % (m/m)
Monoglycerides	0.85	1.35
Diglycerides	0.1	2.74
Triglycerides	0.47	1.91
Free glycerine	0.03	0.05
Total glycerine	0.33	0.9

28.4 Conclusions

Esterification pre-treatment of UCO using various types of ion exchange resins has been investigated. Amongst the catalysts investigated, Purolite D5081 resin showed the best catalytic performance as compared to other two resins, Purolite D5082 and Amberlyst 36. This is probably due to the catalytic properties of this resin, as it has the highest specific surface area and largest total pore volume. At the optimum reaction condition of 60°C reaction temperature, 6:1 methanol to UCO molar ratio, 1.25% (w/w) catalyst loading and 475 rpm stirring speed, Purolite D5081 achieved an FFA conversion of 92%. During the reusability study, the conversion of catalyst dropped by 8-10% after each cycle. Several experiments have been conducted through the homogeneous contribution study, and the results confirmed that resin pore blockage and sulphur leaching were two dominant factors that decrease the catalytic performance of the polymeric resin. For the transesterification reaction, Diaion PA306s catalyst showed the best catalytic performance and the reason was due to the high basicity of the catalyst. As a result, Diaion PA306s was selected for the optimisation study. At the optimum reaction conditions of 9% (w/w) catalyst loading, 328 K reaction temperature, 18:1 methanol to P-UCO feed mole ratio and 350 rpm stirring speed, triglycerides conversion was ca. 75%. The remaining 25% was predicted to be the unreacted triglycerides. During the reusability study, the Diaion PA306s

catalyst gave similar triglycerides conversion after being reused once (at the same conditions). Therefore, it was concluded that the catalyst can be reused several times without losing its catalytic activity. Two types of washing techniques, wet and dry washing, were carried out during the purification process and the results for purified biodiesels were compared with unpurified biodiesel. Biodiesel produced from the dry washing technique shows the lowest percentage of glycerides and glycerine content and therefore was chosen as the best treatment for the purification of biodiesel.

28.5 Acknowledgement

We gratefully acknowledge Purolite International Ltd. (late Dr. Jim Dale and Mr. Brian Windsor) for kindly supplying the catalysts for this research work, Mitsubishi Chemicals for kindly supplying the Diaion catalyst and GreenFuel Oil Co. Ltd. for supplying the UCO. We would like to thank Universiti Malaysia Pahang and Malaysian Government for the Ph.D. scholarship to S.Z.A.

28.6 References

1. Abbaszaadeh, A., B. Ghobadian., M. R. Omidkhah., and G. Najafi. 2012. Current biodiesel production technologies: a comparative review. *Energy Conversion and Management* 63:138-148.

2. Abidin, S. Z. (Supervisors: B. Saha and G.T. Vladisavljević). 2012. Production of Biodiesel from Used Cooking Oil (UCO) using Ion Exchange Resins as Catalysts. PhD Thesis, Loughborough University.

3. Abidin, S. Z., K. F. Haigh., and B. Saha. 2012. Esterification of Free Fatty Acids in Used Cooking Oil Using Ion-Exchange Resins as Catalysts: An Efficient Pretreatment Method for Biodiesel Feedstock. *Industrial and Engineering Chemistry Research* 51: 14653–14664.

4. Abidin, S.Z., D. Patel., and B. Saha. 2013. Quantitative Analysis of Fatty Acids Composition in the Used Cooking Oil (UCO) by Gas Chromatography-Mass Spectrometry (GC-MS). *The Canadian Journal of Chemical Engineering* 91:1896-1903.

5. Atabani, A. E., A. S. Silitonga., I. A. Badruddin, T. M. I. Mahlia., H. H. Masjuki., and S. Mekhilef. 2012. A comprehensive review on biodiesel as an alternative energy resource and its characteristics. *Renewable and Sustainable Energy Reviews* 16:2070-2093.

6. Balat, M. 2011. Potential alternatives to edible oils for biodiesel production – A review of current work. *Energy Conversion and Management* 52:1479-1492.

7. Bianchi, C. L., D. C. Boffito., C. Pirola., and V. Ragaini. 2009. Low temperature de-acidification process of animal fat as a pre-step to biodiesel production. *Catalysis Letters* 134:179-183.

8. David, F., P. Sandra., and A. K. Vickers. 2005. Column Selection for the Analysis of Fatty Acid Methyl Esters. *Agilent Application Notes* 1:5989-3760.

9. Dowd, M. K. 1998. Gas Chromatographic Characterization of Soapstocks from Vegetable Oil Refining. *Journal of Chromatography A* 816:185-193.

10. dos Reis, S. C. M., E. R. Lachter., R. S. V. Nascimento., J. A. Rodrigues Jr., and M. G. Reid. 2005. Transesterification of Brazilian vegetable oils with methanol over ion-exchange resins. *Journal of the American Oil Chemists' Society* 82:661-665.

11. Encinar, J. M., and J. F. González. A. Rodríquez-Reinares. 2007. Ethanolysis of used frying oil. Biodiesel preparation and characterization. *Fuel Processing Technology* 88:513-522.

12. EU Regulation 2568/91. 1991. Official Journal EU, document L248 5/9/1991.

13. EN 1S0 12966-2. 2011. Animal and Vegetable Fats and Oils- Gas Chromatography of Fatty Acid Methyl Esters: Part 2: Preparation of Methyl Esters of Fatty Acids.

14. Falco, M. G., C. D. Córdoba., M. R. Capeletti., and U. Sedran. 2010. Basic ion exchange resins as heterogeneous catalysts for biodiesel synthesis. *Advanced Materials Research* 132:220-227.

15. Feng, Y., B. He., Y. Cao., J. Li., M. Liu., F. Yan., and X. Liang. 2010. Biodiesel production using cation-exchange resin as heterogeneous catalyst. *Bioresource Technology* 101:1518-1521.

16. Haigh, K., G. Vladisavljević., J. C. Reynolds, Z. Nagy., and B. Saha. 2014. Kinetics of the pre-treatment of used cooking oil using Novozyme 435 for biodiesel production. *Chemical Engineering Research and Design* 92:713-719.

17. Haigh, K., S. Z. Abidin., B. Saha., and G. Vladisavljević. 2012. Pretreatment of used cooking oil for the preparation of biodiesel using heterogeneous catalysis. *Progress in Colloid and Polymer Science* 139:19-23.
18. Haigh, K., S. Z. Abidin., G. Vladisavljević., and B. Saha. 2013. Comparison of Novozyme 435 and Purolite D5081 as heterogeneous catalysts for the pretreatment of used cooking oil for biodiesel production. *Fuel* 111:186–193.

19. He, B., Y. Shao., Y. Ren., J. Li., and Y. Cheng. 2015. Continuous biodiesel production from acidic oil using a combination of cation- and anion-exchange resins. *Fuel Processing Technology* 130:1-6.

20. Helfferich, F. 1962. *Ion Exchange*. McGraw-Hill: New York.

21. Ilgen, O. 2014. Investigation of reaction parameters, kinetics and mechanism of oleic acid esterification with methanol by using Amberlyst 46 as a catalyst. *Fuel Processing Technology* 124:134-139.

22. Kaercher, J. A., R. DeCassia., D. S. Schneider. et al. 2013. Optimization of biodiesel production for self-consumption: considering its environmental impacts. *Journal of Cleaner Production*. 46:74-82.

23. Knothe, G., and K. R. Steidley. 2009. A Comparison of Used Cooking Oils: A Very Heterogeneous Feedstock for Biodiesel. *Bioresource Technology* 100:5796-801.

24. Kouzu, M., A. Nakagaito., and J-S. Hidaka. 2011. Pre-esterification of FFA in plant oil transesterified into biodiesel with the help of solid acid catalysis of sulfonated cation-exchange resin. *Applied Catalysis A: General* 405:36-44.

25. Leung, D. Y. C., and Y. Gou. 2006. Transesterification of Neat and Used Frying Oil: Optimization for Biodiesel Production. *Fuel Processing Technology* 87:883-890.

26. Li, J., Y. J. Fu., X. J. Qu., W. Wang., M. Luo., C-J. Zhao., and Y-G. Zu. 2012. Biodiesel production from yellow horn (Xanthoceras sorbifolia Bunge.) seed oil using ion exchange resin as heterogeneous catalyst. *Bioresource Technology* 108:112-118.

27. Lin, L., Z. Cunshan., S. Vittayapadung., S. Xiangqian., and D. Mingdong. 2011. Opportunities and challenges for biodiesel fuel. *Applied Energy* 88:1020-1031.

28. Liu, Y., L. Wang., and Y. Yan. 2009. Biodiesel Synthesis Combining Pre-Esterification with Alkali Catalyzed Process from Rapeseed Oil Deodorizer Distillate. *Fuel Processing Technology* 90:857-862.

29. Liu, X., M. Ye., B. Pu., and Z. Tang. 2012. Risk management for jatropha curcas based biodiesel industry of Panzhihua Prefecture in Southwest China. *Renewable & Sustainable Energy Reviews* 16:1721-1734.

30. López, D. E., J. G. Goodwin Jr., and D.A. Bruce. 2007. Transesterification of triacetin with methanol on Nafion® acid resins. *Journal of Catalysis* 245:381-391.
31. Mazzotti, M., B. Neri., D. Gelosa., A. Kruglov., and M. Morbidelli. 1997. Kinetics of Liquid- Phase Esterification Catalyzed by Acidic Resins. *Industrial & Engineering Chemistry Research* 36:3-10.

32. Özbay, N., N. Oktar., and N. A. Tapan. 2008. Esterification of free fatty acids in waste cooking oils (WCO): Role of ion-exchange resins. *Fuel* 87:1789-1798.

33. Park, J-Y., D-K. Kim., Z-M. Wang., J-P. Lee., S-C. Park., and J-S. Lee. 2008. Production of biodiesel from soapstock using an ion-exchange resin catalyst. *Korean Journal of Chemical Engineering* 25:1350-1354.

34. Pinzi, S., D. Leiva-Candia., I. López-García., M. D. Redel-Macías., and M. P. Dorado. 2014. Latest trends in feedstocks for biodiesel production. *Biofuels, Bioproducts & Biorefining* 8:126-143.

35. Russbueldt, B. M. E., and W. F. Hoelderich. 2009. New sulfonic acid ion-exchange resins for the preesterification of different oils and fats with high content of free fatty acids. *Applied Catalysis A: General* 362:47-57.

36. Shibasaki-Kitakawa, N., H. Honda., H. Kuribayashi., T. Toda., T. Fukumura., and T. Yonemoto. 2007. Biodiesel production using anionic ion-exchange resin as heterogeneous catalyst. *Bioresource Technology* 98:416-421.

37. Shibasaki-Kitakawa, N., T. Tsuji., M. Kubo., and T. Yonemoto. 2011. Biodiesel production from waste cooking oil using anion-exchange resin as both catalyst and adsorbent. *BioEnergy Research* 4:287-293.

38. Shibasaki-Kitakawa, N., K. Hiromori., T. Ihara., K. Nakashima., and T. Yonemoto. 2015. Production of high quality biodiesel from waste acid oil obtained during edible oil refining using ion-exchange resin catalysts. *Fuel* 139:11-17.

39. Silva, V. M. T. M., and A. E. Rodrigues. 2006. Kinetic Studies in a Batch Reactor using Ion Exchange Resin Catalysts for Oxygenates Production: Role of Mass Transfer Mechanisms. *Chemical Engineering Science* 61:316-331.

40. Stamenković, O. S., A. V. Veličković., and V. B. Veljković. 2011. The production of biodiesel from vegetable oils by ethanolysis: Current state and perspectives. *Fuel* 90:3141-3155.

41. Talebian-Kiakalaieh, A., N. A. S. Amin., and H. Mazaheri. 2013. A review on novel processes of biodiesel production from waste cooking oil. *Applied Energy* 104:683-710.

42. Talukder, M. M. R., J. C. Wu., S. K. Lau., L. C. Cui., G. Shimin., and A. Lim. 2009. Comparison of Novozym 435 and Amberlyst 15 as Heterogeneous Catalyst for Production of Biodiesel from Palm Fatty Acid Distillate. *Energy & Fuels* 23:1-4.

43. Tesser, R., M. Di Serio., M. Guida., M. Nastasi., and E. Santacesaria., 2005. Kinetics of oleic acid esterification with methanol in the presence of triglycerides. *Industrial & Engineering Chemistry Research* 44:7978-7982.

44. Yaakob, Z., M. Mohammad., M. Alherbawi., Z. Alam., and K. Sopian. 2013. Overview of the production of biodiesel from Waste cooking oil. *Renewable and Sustainable Energy* Reviews 18:184-193.

45. Yadav, G. D., and H. B. Kulkarni. 2000. Ion-exchange resin catalysis in the synthesis of isopropyl lactate. *Reactive and Functional Polymers 44*:153-165.

46. Zhang, J., and L. Jiang. 2008. Acid-catalyzed esterification of Zanthoxylum Bungeanum seed oil with high free fatty acids for biodiesel production. *Bioresource Technology* 99:8995-8998.